UNIVERSIDADE NOVA DE LISBOA

Faculdade de Ciências e Tecnologia

Departamento de Química

IMPERIAL COLLEGE OF LONDON

Faculty of Engineering

Chemical Engineering Department

Development of Polymeric Membranes for Forward Osmosis

Por

Filipa Cristina Conceição Alves

Dissertação apresentada na Faculdade de Ciências e Tecnologia da Universidade Nova de Lisboa para obtenção do grau de Mestre em Engenharia Química e Bioquímica.

Supervisor: Professor Andrew Livingston e Professora Isabel Coelhoso

Co-Supervisor: Dr. Sairam Malladi

Lisboa

(2010)

Acknowledgements

I would like to express my gratitude to the following people, for helping me in the accomplishment of this work:

- *Professor Andrew Livingston (Imperial College London)*
- *Postdoc. Sairam Malladi (Imperial College London)*
- *Professora Isabel Coelhoso (Faculdade de Ciências e Tecnologia)*
- *My family and friends*
- *All Andrew's Group*

Abstract

Forward osmosis (FO) using a semi-permeable membrane may be a viable alternative to reverse osmosis (RO) as a lower cost and more environmentally friendly desalination technology. To develop a FO membrane showing high water flux and high salt rejection, P84 Lenzing polyimide flat sheet membranes were fabricated by immersion precipitation from a casting solution containing dimethylformamide (DMF) as the solvent and 1,4-Dioxane (dioxane) as the co-solvent.. Different P84 concentrations as well as different solvent systems compositions were tried. The composition of the solvent system showed to provide control over the molecular weight cut-off and porosity of the resultant membranes. High water flux (2.18 $kg.m^{-2}.h^{-1}$) and improved salt rejection (95.2%) in FO were achieved by using 18 wt.% P84, DMF:Dioxane, 1:6, crosslinked for 4h by 1,6-Hexanediamine (HDA). Glycerol and Polyethylene glycol (MW 400 $g.mol^{-1}$) (PEG) were used to store membranes after casting in order to prevent pores collapse. The best membrane fabricated, 18 wt.% P84, DMF:Dioxane, 1:6, showed better performance when stored in PEG than when stored in glycerol. Internal concentration polarisation is thought to be the cause for the experimental FO water fluxes, which were far lower than those theoretically predicted based on bulk osmotic pressure difference and membrane pure water permeability data.

List of abbreviations

CA	Celulose Acetate
CP	Concentration polarisation
CTA	Cellulose triacetate
DMF	Dimethylformamide
DMSO	Dimethyl sulfoxide
ECP	External concentration polarisation
ESR	Einstein-Stoke radius
FO	Forward Osmosis
HDA	1,6-Hexanediamine
HTI	Hydration Technologies Inc
ICP	Internal concentration polarization
MD	Membrane Distillation
MDI	4,4'-methylenebis (phenyl isocyanate)
MED	Multi-effect distillation
MSF	Multistage flash
MW	Molecular weight
NF	Nanofiltration
PAH	Poly(amide hydrazide)
PEG	Polyethylene glycol
PES	Polyethersulfone
PI	Polyimide
PRO	Pressure-retarded osmosis
PVP	Polyvinylpyrrolidone
RO	Reverse Osmosis
TDI	2-methyl-m-phenylene diisocyanate
TFC	Thin-film composite

THF	Tetrahydrofuran
VC	Vapour condensation
ZLD	Zero-liquid discharge

Numenclature

$c_{1,0}$	Solvent concentration in feed side of membrane.
d_p	Membrane pore size.
r_p	Pore size
r_s	Solute Einstein-Stokes radius (ESR).
t	Thickness
w_i^*	Mass fraction of solvent in membrane at equilibrium swelling.
w_m	Logarithmic average of the mass fraction of solvent at the Upstream side and at the downstream side.
A	Area of membrane.
$C_{2,1}^S$	Solute concentration downstream solution.
$C_{2,0}^S$	Solute concentration upstream solution.
C_f	Solute concentration on the feed side of the membrane.
C_p	Solute concentration on the permeate side of the membrane.
C_r	Solute concentration on the retentate.
$D_{1,m}$	Multi component diffusion coefficient of solute versus membrane.
$D_{2,m}$	Multi component diffusion coefficient of solute.
D_{im}	Multi component diffusion coefficient of solvent.
D_s	Diffusion coefficient of the solute.
E	Phenomenological coefficient.
J_i	Flux of the component i.
J_w	Water flux.

k	Permeability constant.
K	Resistance to solute diffusion within the membrane porous support layer.
K_1	Solvent sorption.
K_2	Solute distribution coefficient.
M_i	Molecular weight of the component i.
P	Membrane permeability.
R	Solute rejection.
R_g	Gas constant.
T	Temperature.
v_i	Diffusive volume flux of a species i
V	Volume of permeate.

Greek Symbols

Π_{Hi}	Osmotic pressure of the bulk draw solution.
Π_{Low}	Osmotic pressure of the bulk feed solution.
$\Delta\pi$	Osmotic pressure difference.
ΔP	Pressure difference.
$\Delta Weight$	Weight variation in the draw solution after FO run.
ρ	Mass density of the membrane.
ε	Porosity.
σ	Reflection coefficient.

σ_g Geometric standard deviation about the mean ESR.

σ_p Geometric standard deviation about the membrane mean pore size.

η Solvent viscosity.

τ Tortuosity.

μ_p Membrane mean pore size.

μ_s Solute Einstein-Stokes radius of the “mean” solute.

Table of Contents

List of figures

List of tables

Introduction

The U.S Geological Survey found that 96.5% of Earth's water is located in seas and oceans while 1.7% in located in the icecaps and less that 0.8% is considered to be fresh water. The remaining percentage corresponds to brackish water found in estuaries and aquifers. As a result, about 2.3 billion of people (41% of world population) live in regions suffering of water scarcity and over 1 billion people are without clean drinking water [1]. Additionally, the traditional potable water resources, such as rivers, lakes and groundwater, are being exhausted by the fast world population growth and continue development of countries. As a result, these resources are diminishing or becoming saline. Therefore, even the countries that do not face water shortages at the moment may have this problem in a near future. Thus, the production of potable water has become a worldwide concern. Water reuse and water desalination have emerged as possible solutions to this matter. Water reuse only provides water for uses, such as irrigation, plant cooling water and groundwater recharge. On the other hand, water desalination has become an important source of potable water production, since seawater is a virtually unlimited water resource.

Desalination processes include two main categories: Thermal processes, such as distillation, that have been developed over the past 60 years, and pressure-driven membrane processes, such as reverse osmosis (RO), developing over the past 40 years. Reverse osmosis has rapidly developed since the 1960s and it has become the most popular method to desalinate water, due to its lower energy requirements, minimal usage of chemicals and reduced occupied area in comparison to thermal processes. However, those have remained the primary technology of choice in the Middle East, where fossil fuel resources are abundant and easy to access.

Despite these several advantages, challenges are still to overcome in the field of water desalination. The high pressures applied in RO results in high energy consumption as well as aggressive fouling phenomenon, which in turn make compulsory membranes replacement very often (2-5 years) [2], with considerable associated costs. Moreover, the concentrated brine obtained after RO is discharged back into the sea, causing serious damages to marine environment.

Recently, a new method to desalinate water has drawn scientific community attention. This method is called Forward Osmosis (FO) and it is also a membrane process. However, unlike RO that uses an applied pressure as the driving force for mass transport through the membrane, FO uses only osmotic pressure as the driving force for mass transport. This osmotic gradient in FO is achieved by placing a higher osmotic pressure solution ("draw" solution) on the permeate side of the membrane. The permeated water is later recovered from this solution. Therefore, the energy consumption in FO will be certainly lower. Other advantages of FO process may be reduced fouling phenomenon, due to low pressures applied as well as possible elimination of pre-treatment stage, compulsory required in RO.

However, FO current technology has not yet reached the potential benefits of the method. Improvements on FO system, particularly in “draw” solution choice and in membrane performance remain to be done.

This work explores the fabrication of FO flat sheet membranes using polyimide (P84 Lenzing) and its performance in FO process.

Polyimides membranes have been fabricated to be employed in reverse osmosis and nanofiltration processes for its excellent thermal and chemical stability as well as its high selectivity and thin film formability [3,4].

1. Literature Review

1.1. Membrane technology

Membrane technology has been successfully applied in several separations processes including pharmaceutical, food, wastewater and petrochemical industries.

Compared with traditional separation processes, membranes are an easy-to-operate and low-maintenance process. They can be disposed in modules which can be added to achieve the desired separation, thus its scale-up is simple. These systems usually have low capital cost, compact size and low power consumption, which reduce the production cost. Membrane technology also has a trend in being more energy efficient than the conventional techniques as well as being cleaner, therefore more environmentally friendly.

1.1.1. What is a membrane?

A membrane is defined as a selective barrier between two phases which restricts the transport of some substances and allows the transport of others from one phase to another.

A membrane can be homogeneous or heterogeneous, symmetric or asymmetric in structure, solid or liquid; can carry positive or negative charge or be neutral or bipolar.

The principal types of membranes are shown schematically in Figure 1.

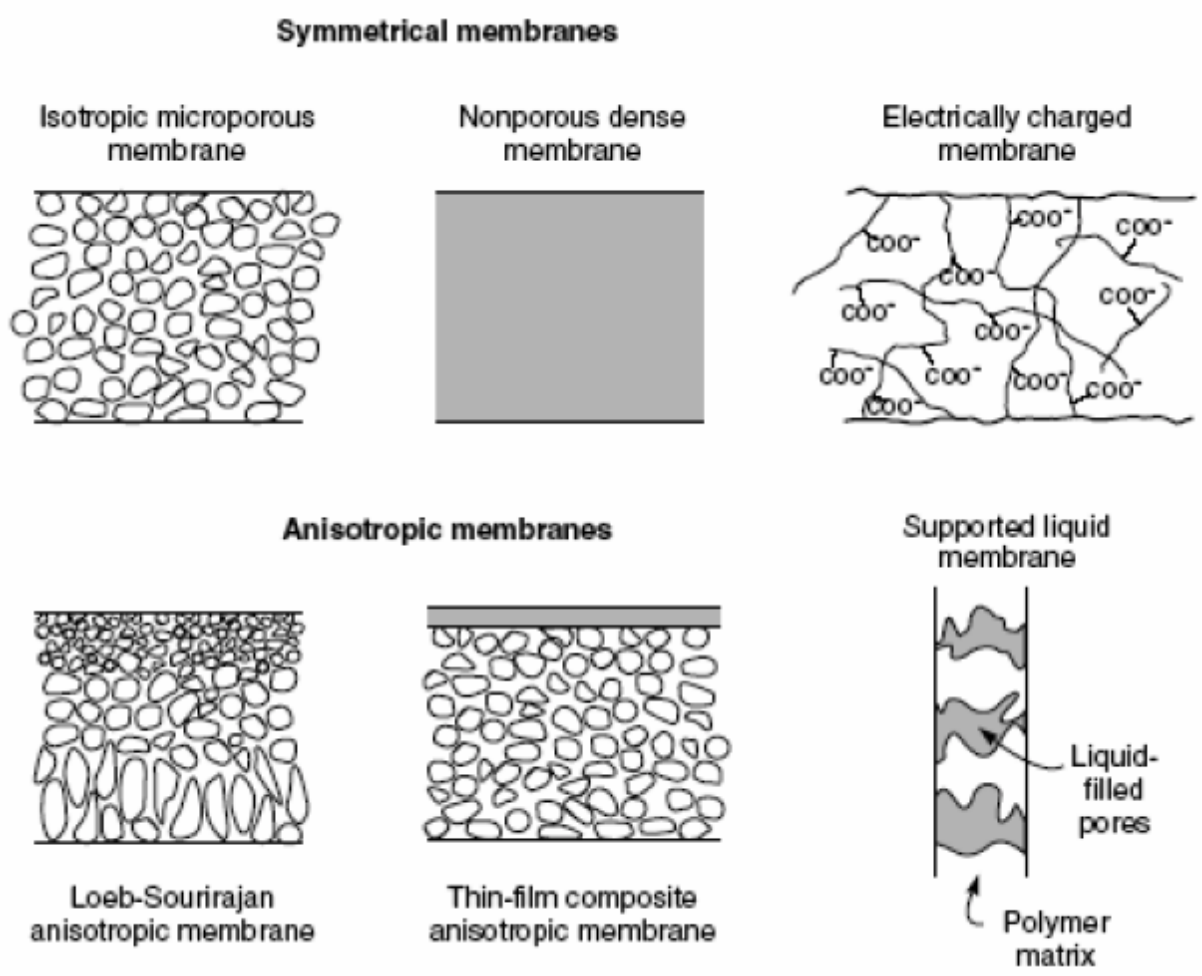

Figure 1 – Schematic diagrams of principal types of membranes [5].

Thus, membranes can be classified as:

- Isotropic membranes: Microporous membranes, nonporous dense membranes and electrically charged membranes, which influences the transport of charged particles.
- Anisotropic membranes.
- Ceramic, metal and liquid membranes.

The porous membranes are usually used in filtration processes, where separation is made by particle size. Nonporous membranes are frequently used in pervaporation and gas separation processes, where the separation occurs according to the difference in solubility and diffusivity of the molecules in membrane material.

In some cases the transport through the membrane is not determined by its structure or material but only by a specific carrier-molecule, which facilitates the transportation of a certain component. Since the transportation of a component is just dependent on its carrier specificity, high selectivity can be achieved using the most specific carrier. The carrier molecule can be incorporated on membrane matrix or be mobile when dissolved in a liquid.

As can be seen from the picture, anisotropic membranes consist of a dense skin-layer and porous sublayer. The dense skin-layer is the functional portion of the membrane providing its selectivity, whereas the porous sublayer provides higher flux, so unlike symmetric membranes, anisotropic membranes can combine high selectivity with high [6].

The Loeb-Sourirajan membrane, also known as asymmetric integrally skinned membrane, possesses a skin-layer on the top of a porous sublayer with the same composition. However, in thin-film composite (TFC) membranes the skin-layer and the porous sublayer are made of different materials, which mean that the active layer and porous sublayer can be independently optimized to maximize the overall membrane performance.

Integrally skinned membranes have considerably lower manufacturing costs than TFC membranes. For this reason, this was the type of membrane I studied. A special attention will be given to these from now onwards.

1.1.2. Membrane processes

Transport through the membrane takes place when a driving force is applied on the components of the feed. The driving force can be pressure, concentration (activity), temperature or electrical potential difference across the membrane. All driving forces can be included in one parameter, chemical potential [7]. The membrane processes according to their driving forces can be seen in the next table.

Table 1- Classification of membrane processes according to their driving forces [7].

Pressure difference	Concentration (activity) difference	Temperature difference	Electrical potential difference
Microfiltration	Gas separation	Membrane distillation	Electrodialysis
Ultrafiltration	Pervaporation		
Nanofiltration	Carrier mediated transport		
Reverse Osmosis	Dialysis		
Piezodialysis	Diffusion dialysis		

1.1.3. Transport in membranes

The flux of a certain component through a membrane is proportional to the driving force applied. This relation can be expresses by the fallowing equation.

$$J_i = E \times \frac{dX}{dx} \quad \text{Eq. 1}$$

Where J_i is the flux of the component i and dX/dx is the driving force expressed as a gradient (of pressure, concentration, etc.) X along a coordinate x perpendicular to the selective barrier. E is called the phenomenological coefficient [7].

At the moment, two main models are commonly used to describe transport in membranes: pore-flow model and solution-diffusion model. In both models, the difference in pressure across the membrane establishes the chemical potential gradient.

Pore-flow model

The pore-model assumes that different permeants are separated through tiny pores in the membrane by size-exclusion. The pore-flow mechanism also supposes that the concentration of solute and solvent is constant along the membrane. Thus, the transport through porous membranes can be described based on hydrodynamic analysis by Darcy's law (Eq.2) in which l is the membrane thickness and k is the permeability coefficient, that contains membrane structural factors as membrane pore size (r_p), porosity (ε) and tortuosity (τ) and solvent viscosity (η) [8].

$$J = k\frac{\Delta P}{l}, where\ k = \frac{\varepsilon r_p}{8\eta\tau} \quad \textbf{Eq. 2}$$

Solution-diffusion model

The solution-diffusion was initially used to explain transport of gases across polymeric film and nowadays it became the most widely accepted explanation of membrane transport mainly in dialysis, reverse osmosis, gas permeation and pervaporation operations. This model assumes that permeants dissolve in the membrane material and then dissolve through the membrane due to a concentration gradient. The separation between different permeants occurs due to differences in their solubilities and diffusivities properties [8]. The solution-diffusion mechanism is described by Eq.3.

$$J_i = \frac{K_i D_{im}}{l}\ \ 1 - e^{\frac{-V_i\ \Delta p - \Delta\pi}{R_g T}} \quad with\ K_i = \frac{\rho w_i^*}{w_m M_i} \quad \textbf{Eq. 3}$$

Equations for solute and solvent respectively, were also derived from this model:

$$J_1 = \frac{D_{1,m} K_1 c_{1,0} (\Delta p - \Delta\pi)}{l R_g T} \quad \textbf{Eq. 4}$$

$$J_2 = \frac{D_{2,m} K_2}{l}\ \ C_{2,o}^S - C_{2,l}^S \quad \textbf{Eq. 5}$$

Solute transport model

This model is often used to characterize porous membranes in terms of mean pore size and pore size distribution. The model is based on the following assumptions [9-11].

- The Stokes-Einstein radius can represent the size of a solute molecule.
- The size and the shape of a solute molecule do not depend on whether the solute is in the bulk solution or in the membrane pore.

- The transport of a solute molecule in not affected by the interaction force working between the solute and the membrane.
- Size exclusion is the only mechanism for solute separation.

Solute rejection, R in percentage is defined as

$$\%R = \left(1 - \frac{C_p}{C_F}\right) \times 100 \quad \textbf{Eq. 6}$$

Where C_p and C_f are the solute concentrations in the permeate and in the bulk of feed solutions. When solute rejection (%) of a porous membrane is plotted against the solute Einstein-Stoke radius (ESR) on a log-normal probability paper, a straight line is yielded as reported by [9]. If solute rejection correlates with solute diameter according to the log-normal probability function, then the following relationship is obtained:

$$R = \text{erf } z = \frac{1}{\sqrt{2\pi}} \int_{-\infty}^{z} e^{-\frac{u^2}{2}} du, where\ z = \frac{lnr_s - ln\mu_s}{ln\sigma_g} \quad \textbf{Eq. 7}$$

Where r_s is the solute ESR, μ_s is the ESR of the "mean" solute at R=50% and σ_g is the geometric standard deviation about the mean ESR.

From the log-normal plot, mean solute size (μ_s) can be calculated as r_s corresponding to R=50% and σ_g can be determined from the ratio of r_s at R=84.13% and at 50%. By ignoring the dependence of solute rejection on the steric and hydrodynamic interaction between solute and pore sizes, the mean pore size (μ_p) and the geometric standard deviation (σ_p) of the membrane can be considered to be the same as of solute mean size and solute geometric standard deviation [10, 12-14].

From μ_p and σ_p the pore size distribution of a porous membrane can be expressed by the following probability density function:

$$\frac{df(d_p)}{dd_p} = \frac{1}{d_p ln\sigma_p \sqrt{2\pi}} exp\left(-\frac{(lnd_p - ln\mu_p)^2}{2(ln\sigma_p)^2}\right) \quad \textbf{Eq. 8}$$

Where d_p is the pore size.

The relationship between ESR, r_s and molecular weight (MW), of neutral solutes can be expressed by the following equation [15,16]:

$$logr_s = -1.4962 + 0.4657\ logMW \quad \textbf{Eq. 9}$$

1.1.4. Membrane processes drawbacks

The performance of membrane operations is reduced by two main phenomena, concentration polarisation and fouling.

Concentration Polarisation

Concentration polarisation (CP) is the accumulation of solutes at the membrane active layer surface as a result of a permeate flow through the membrane. It creates a higher solute concentration at the membrane surface compared with bulk. This phenomenon has greater effects in pressure-driven processes due to high pressures used. In such processes CP leads to flux reduction due to increased pressure that must be overcome.

Membrane fouling

Membrane fouling is the process in which feed substances are retained onto or into the membrane pores causing severe flux decline. Fouling includes solute adsorption and cake-layer formation on membrane surface. Severe membrane fouling may require chemical cleaning or worse membrane replacement. Thus fouling constitutes the major problem in membrane technology.

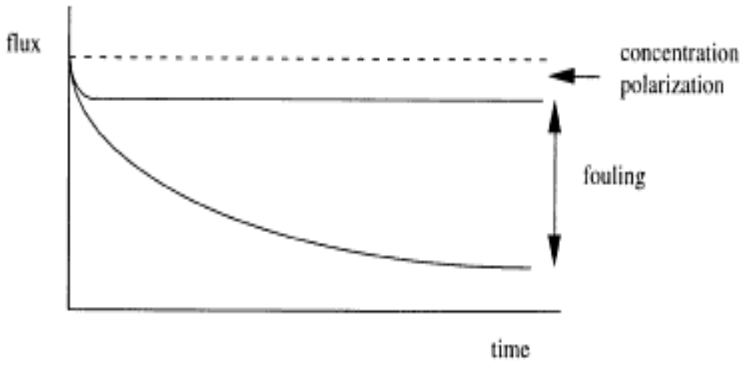

Figure 2- Effect of fouling and concentration polarisation on flux [7].

1.2. Membrane materials

Several materials can be used to prepare membranes. These materials can either be inorganic such as ceramic, glass, metal or organic, including all kind of polymers [7]. The material selection for membranes is based on film forming properties, chemical and thermal stability, commercial availability, price and affinity for feed components. Membranes for industrial application require reproducibility performance as well as long-term stability and cleanability. Ceramic membranes show superior performance in terms of chemical and thermal stability, they are also easier to clean and do not deform under pressure nor do they swell. However, one of the drawbacks of ceramic membranes is their scale-up, since they tend to be more brittle and expensive than polymeric membranes. Thus, most of the commercial available membranes are polymeric [8].

1.3. Membrane preparation

The technique to employ in order to prepare a membrane will depend on the chosen material, which in turn will depend on the final application of the membrane.

Polymeric membranes can be obtained by several techniques such as sintering, stretching, track-etching and phase inversion, which is a technique that was developed by Loeb and Souriranjan [17] in the early sixties and represents one of the most economical and reproducible techniques to prepare polymeric asymmetric integrally skinned membranes.

1.3.1. Phase inversion

All methods for preparing phase inversion membranes involve the precipitation of a polymer-rich phase from an initial homogeneous polymer solution. The precipitation process is initiated by the transition from the homogeneous solution phase into two phase systems, a polymer-rich phase which forms the membrane structure and a polymer-poor phase which forms the membrane pores. The initial stage of phase transition determines the membrane morphology (i.e porous or non-porous). Phase inversion membranes can be performed by several techniques such as precipitation by solvent evaporation, precipitation from the vapour phase, precipitation by controlled evaporation, thermal precipitation and immersion precipitation [7,18].

Nowadays, immersion precipitation is the most applied technique to prepare membranes, since it is economical, reproducible and can be applied to a wide variety of polymers.

Immersion precipitation

Immersion precipitation process uses at least three components: a polymer, a solvent to the polymer and a non-solvent to the polymer, whereas, the solvent and the non-solvent must be completely miscible with each other. Water is often used as a non-solvent since usually it does not dissolve polymers and is harmless to the environment. However, other organic solvents can also be used.

Immersion precipitation membranes are prepared in the fallowing way: A polymer is dissolved in a suitable solvent or mixture of solvents that can include additives. Later the polymer solution (also referred to as casting solution or dope solution) is cast as a thin film upon a supporting layer, (commonly a nonwoven backing as polypropylene/polyethylene or polyester) and then immersed in a non-solvent bath. In the non-solvent bath the solvent diffuses into the coagulation bath whereas the non-solvent diffuses into the cast film [7].

After a given period of time the solution becomes thermodynamically unstable due to the exchange of solvent and non-solvent and liquid-liquid demixing occurs. In the end the polymer precipitates and a solid polymeric film with an asymmetric structure is obtained.

Phase separation occurs initially at the surface of the cast polymeric film. Due to the low polymer chemical potential at the surface, a net movement of polymer in the direction perpendicular to the surface occurs, which leads to an increase of the polymer concentration at the surface layer. This concentrated surface layer will originate the skin-layer of the integrally skinned membranes. Once, the skin-layer is

formed, it is going to act as a limiting barrier for precipitant transport into the casting solution and so the concentration profiles in the interior of the casting solution become less steep and a randomly distributed polymer structure is obtained, constituting the membrane sublayer [7,18,19].

The membranes obtained after precipitation can be used directly or a post treatment can be applied (e.g. heat treatment).

Liquid-liquid demixing process

The exchange that occurs between the solvent and the non-solvent during the phase inversion process is referred to as liquid-liquid demixing and plays an important role in the resulting morphology of the membrane.

The liquid-liquid demixing process is often illustrated by a ternary phase diagram as the one shown in Figure 3.

The corners of the triangle represent pure components, polymer, solvent and non-solvent. A point on one of the sides of the triangle represents a mixture of the two corner components whereas a point within the triangle represents a mixture of the three components. The triangle consists of two regions separated by a binodal curve: A one-phase region (I) where all the components are miscible and a two phase-region (II) where the system separates into a polymer-rich phase and a polymer-poor phase. In the binodal curve these two coexisting phases are in equilibrium with each other.

The composition of the system during the precipitation process is illustrated by the arrowed path A to C, during which the solvent is exchanged by the non-solvent. Composition A represents the initial casting solution (thermodynamically stable) free of non-solvent. By contacting with a certain amount of non-solvent this solution starts getting unstable. When the binodal is reached liquid-liquid demixing occurs and the precipitation is initiated (point B on the path). As the solvent is lost during the precipitation process, the polymer rich phase becomes more and more viscous and at some point its viscosity is high enough that the polymer solidifies (point D on the path).The further solvent/non-solvent exchange results in the shrinkage of the polymer-rich phase forming the final membrane (point C on the path). At composition C two phases are in equilibrium, a solid (polymer-rich) phase which constitutes the final membrane structure and a liquid (polymer-poor) phase which constitutes the membrane pores filled with non-solvent. The position of point C determines the overall porosity of the membrane [19].

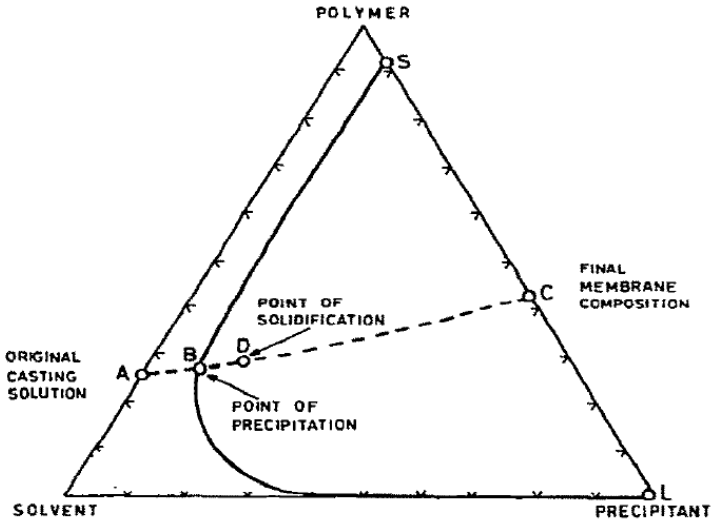

Figure 3- Schematic phase diagram of the system polymer-solvent-precipitant showing the precipitation pathway of the casting solution during membrane formation [19].

Two main types of demixing process can be distinguished: instantaneous liquid-liquid demixing and delayed onset of liquid-liquid demixing. Instantaneous liquid demixing means that the membrane is formed immediately after immersion in the non-solvent bath whereas in the case of delayed demixing it takes some time before the membrane is formed. The two types of demixing are illustrated in a ternary phase diagram in Figure 4.

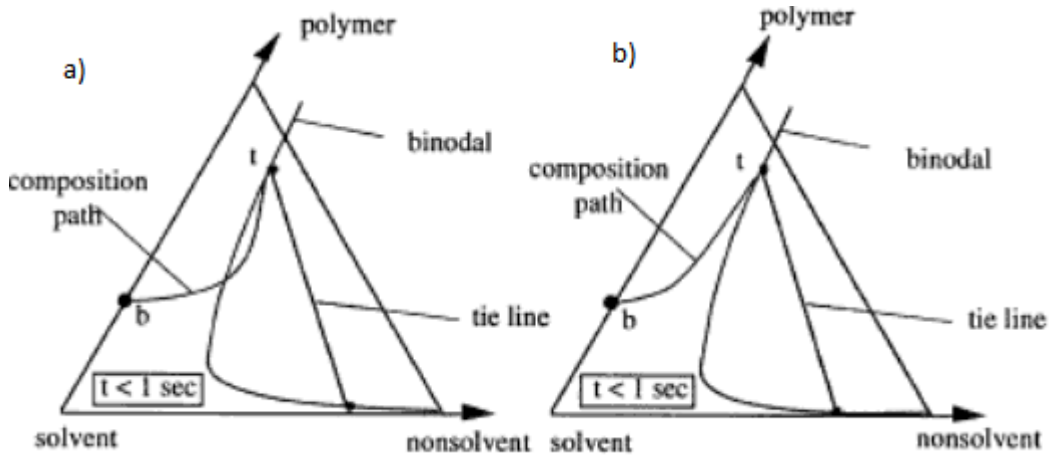

Figure 4- a) Instantaneous liquid-liquid demixing; b) delayed liquid-liquid demixing [7].

Figure 4 illustrates a composition path of a cast film at the moment of its immersion in the non-solvent bath (t <1 sec). Point t gives the composition at the top of the film, while point b gives the composition of the bottom. In Figure 4 a) the composition path has already crossed the binodal curve, which indicates that the liquid-liquid demixing has started immediately after immersion whereas in Figure 4 b) all the path

compositions still in the one-phase region indicate that the liquid-liquid demixing has not yet started [7].

A phenomenon often associated with instantaneous demixing during immersion precipitation is the formation of macrovoids, finger-like pores that can extend over all membrane thickness. In high pressure applications the presence of macrovoids in large number can result in compaction or collapse of polymeric membranes, which in turn reduces the flux [20].

Generally, instantaneous liquid-liquid demixing promote the formation of porous membranes (microfiltration and ultrafiltration membranes), while delayed liquid-liquid demixing promote the formation of dense membranes (gas separation and pervaporation membranes) [7,20,21].

1.4. Factors affecting membrane structure

1.4.1. Addition of solvent to the coagulation bath

The addition of solvent to the coagulation bath delays the liquid-liquid demixing during phase inversion influencing strongly the membrane structure obtained.

The maximum amount of solvent that can be added to a coagulation bath is determined by the position of the binodal curve in the ternary phase diagram. The closer the binodal curve is to the polymer/solvent axis, the faster the demixing. Consequently, a higher the amount of solvent is permitted in the non-solvent bath [7,19].

1.4.2. Solvent/nonsolvent system

Altena et al. [22] claimed that when the miscibility between the solvent and the non-solvent increases, instantaneous demixing during phase inversion occurs.

Reuvers in his phD thesis [23] studied the system cellulose acetate (CA)/solvent/water, using as solvents THF, acetone, dioxane, DMF and DMSO. The miscibility of these solvents with water decreases following the order THF > acetone > dioxane > DMF > DMSO. During his experimental work he noted that when DMSO, DMF and dioxane were used as a solvent, instantaneous demixing occurred, whereas using THF a delayed demixing occurred. In order to delay the observed liquid-liquid demixing he added a certain amount of the respective solvent to the non-solvent bath. And he observed that the higher the miscibility with water (non-solvent) the higher the amount of solvent required in the water bath to delay the liquid-liquid demixing process (Figure 5).

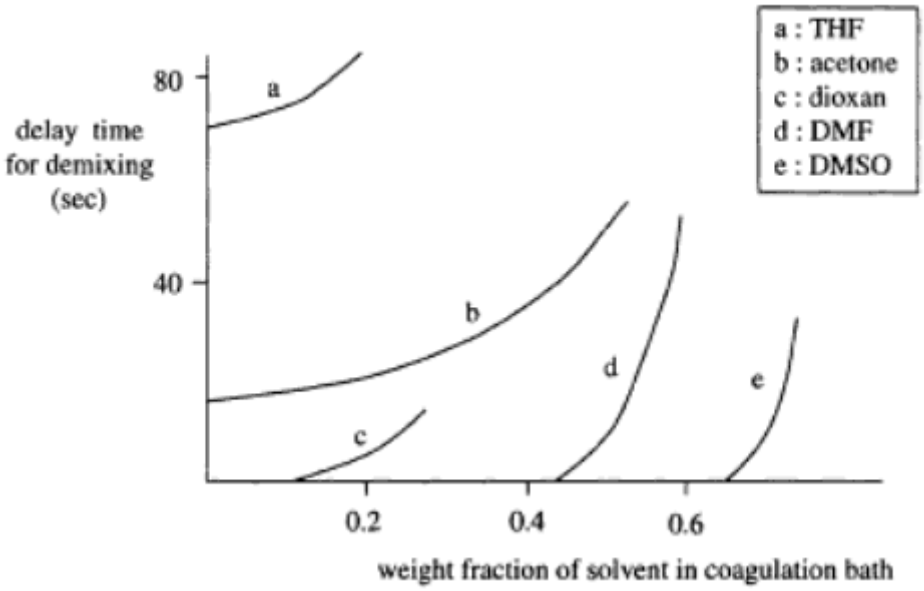

Figure 5- Influence of the amount of solvent present in coagulation bath on the delay time for demixing [7].

In short, when a high affinity between the solvent and the non-solvent exists a porous membrane is obtained; whereas when this affinity is low, a membrane with a dense non-porous top layer is obtained.

1.4.3. Polymer concentration

Increasing polymer concentration in the casting solution result in a more concentrated interface casting solution/non-solvent during phase inversion, which slows down the solvent/non-solvent exchange leading to delayed demixing. Therefore, the resulting membranes show denser skin-layers and sublayers [7,8].

1.4.4. Addition of non-solvent to the casting solution

In the same way that the addition of non-solvent to the coagulation bath delays the liquid-liquid demixing during phase inversion, the addition of non-solvent directly to the casting solution also delays the liquid-liquid demixing. However, when the non-solvent is added to the casting solution the composition of the system polymer/system of solvents (where the system of solvents consists of solvent/non-solvent), must remain in the one-phase region in the ternary phase diagram, this means that all the system components must remain completely miscible with each other.

Yoong Hsiang See-Toh et al. [21] carried out several experiments using polyimide P84 as the polymer and DMF as the solvent and 1,4 dioxane as the non-solvent added to the casting solution. They observed that the higher the amount of dioxane added to the dope solutions the fewer the finger-like structures in the resulting membranes. This was a result of delayed demixing during phase inversion.

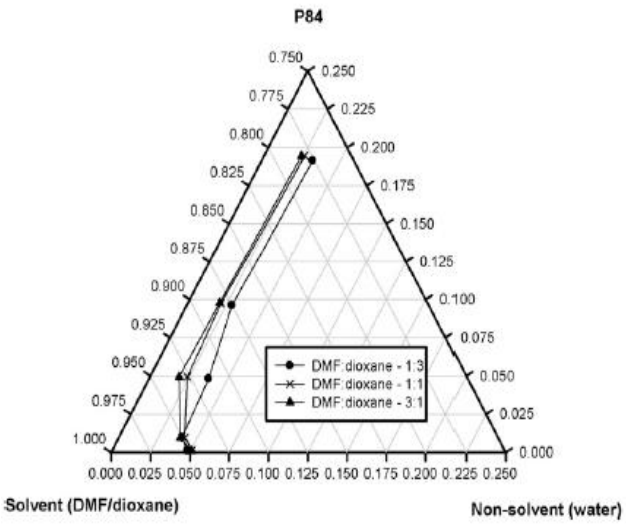

Figure 6- Ternary diagram of P84 at different DMF:Dioxane compositions at 25 ºC [21].

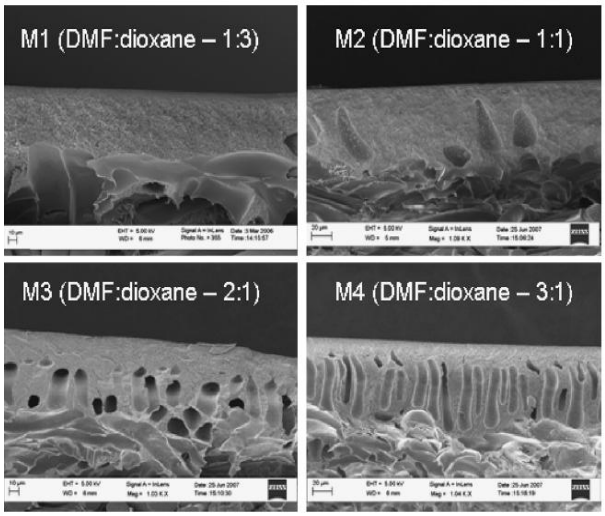

Figure 7- Cross-section SEM pictures of the seperation layer of membranes prepared from 22 wt.% P84 with different DMF:Dioxane ratios in the dope solution [21].

1.4.5. Evaporation time

The evaporation is defined as the elapsed time from the beginning of casting to the instant at which the cast polymer film enters the precipitation bath.

Fritz et al. [20] conducted several experiments using CA/acetone system and precipitation bath consisting of water. Membranes were casted at different polymer concentrations and at different thicknesses. The results showed that macrovoids structures could be completely suppressed by increasing the duration of the evaporation step or by decreasing the initial casting solution thickness sufficiently.

The evaporation step also increases the polymer concentration in the polymer film surface during phase inversion and consequently favours the onset delayed demixing that usually suppresses macrovoids formation.

1.4.6. Pore-forming additives

Inorganic salts such as LiCl and $LiNO_3$ and organic compounds such as polyethylene glycol (PEG) and polyvinylpyrrolidone (PVP) have been added to casting solutions in order to enhance the porosity in the resulting membranes.

Mohamad et al. [24] noticed that the addition of LiCl and $LiNO_3$ to casting solutions of poly(amide hydrazide) (PAH) promoted an enhancement in membrane permeability without lowering its selectivity.

1.5. Membrane post-treatment

Membrane post-treatment is often applied to enhance the membrane separation performance as well as to increase its long-term stability.

1.5.1. Annealing

During phase inversion process, the polymer precipitation is usually fast and as a result a highly dispersed polymer structure far from its thermodynamic equilibrium is obtained [25].

Thermal annealing of a polymeric membrane facilitates the rearrangement of its polymeric chains towards the thermodynamically favoured structure [25].

The conformational motions of the polymer chains during thermal annealing procedure often lead to membrane densification and shrinkage, increasing its selectivity and simultaneously reducing its permeability. Additionally, membrane annealing also enhances its physical strength [25,26].

1.5.2. Crosslinking

Membranes can be crosslinked in order to enhance their chemical stability and rejection properties. Membrane crosslinking can be chemical, photo-induced or plasma and always result in a reduction in membrane permeability [8].

1.5.3. Drying by solvent exchange

In order to minimize the risk of pore collapse upon drying, the non-solvent present in membranes after immersion is usually replaced by a first solvent (miscible with the non-solvent). This one is then replaced by a second solvent, more volatile, that is easily removed by evaporation in order to obtain the dry membrane.

The enhancement of membranes flexibility and handling, required for their transportation, can also be achieved by impregnating them with conditioning agents such as lube oils, glycerol or long chain hydrocarbons [8].

1.6. Water desalination process

Desalination is a water-treatment process that removes salts from water providing fresh water not only from ocean, but also from saline ground water, which is very important in countries as Mexico where 75% of ground water is too saline for most uses without treatment.

Thermal distillation is the oldest method to obtain drinking water from seawater. It was first developed for commercial use aboard ships. Thermal distillation enabled sailors to travel for longer periods of time by suppressing the need of carrying fresh water onboard. In the 17th century, Japanese sailors used a simple distillation technique, where water was boiled in pots and the evaporated water collected in bamboo tubes [1].

1.6.1. Current technology

Desalination methods include two main processes: Phase separation processes (thermal methods) or single phase processes (membrane processes).

The most commonly used thermal methods are multi-effect distillation (MED), multistage flash (MSF) and vapour condensation (VC) while the most used membrane method is reverse osmosis (RO) [27].

In thermal methods water is usually heated at lower pressure until evaporation, meaning separation from the salt. In RO process a hydraulic pressure is applied to the feed water creating a driving force for water permeation through the membrane, which restricts salt molecules passage.

The cost of water produced (per m^3) by thermal and membrane processes can be seen bellow:

Table 2- Typical average capacity and corresponding water cost for different desalination technologies [27].

Desalination method	Size of plant (m^3/day)	Cost (per m^3)
MED	>91,000	0.42 – 0.81
MSF	23,000-528,000	0.42-1.40
VC	1000-1200	1.61-2.13
RO	100,000 – 320,000	0.36-0.53

Thermal methods are more expensive once they require large quantities of fuel to vaporize salt water, while RO process just uses electric energy. Since RO is more energy-saving, suppresses the usage of chemicals and occupies less space for a given capacity of production it has replaced thermal methods in brackish and seawater desalination.

Today, over 15,000 desalination plants are in operation around the world, and about 50% of those are RO plants. The Middle East holds approximately 50% of world's production capacity with Saudia Arabia being the world leader, holding about 26% of global production capacity. United States ranks in second, with 17% of the world's desalination capacity. The distribution of desalination production capacity for different separation techniques is shown in Figure 8 for the entire world, the United States and Saudi Arabia. Membrane processes include also nanofiltration (NF) and electrodialysis (ED) **[1].**

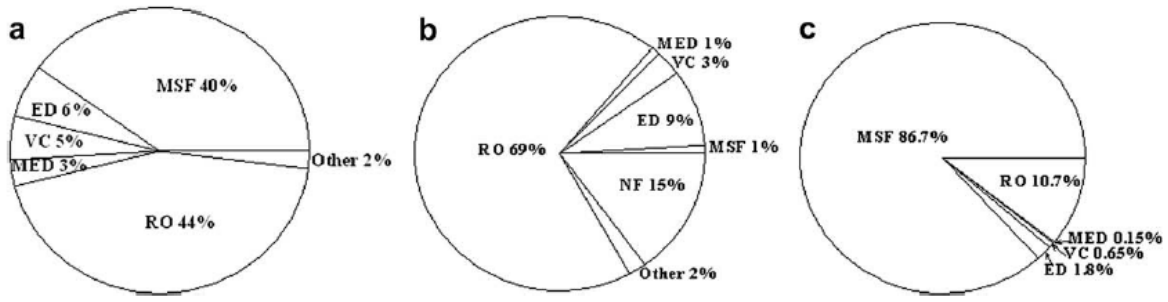

Figure 8- Distribution of desalination production capacity by process technology for (a) the world, (b) the United Stated, and (c) the Middle East (countries include Saudi Arabia, Kuwait, United Arab Emirates, Qatar, Bahrain, and Oman) [1].

RO membranes materials

There are two major groups of polymeric materials which have been used to produce satisfactory reverse osmosis membranes: cellulose acetate and composite polyamide. The structures of cellulose acetate and polyamide are shown in Figure 9, bellow.

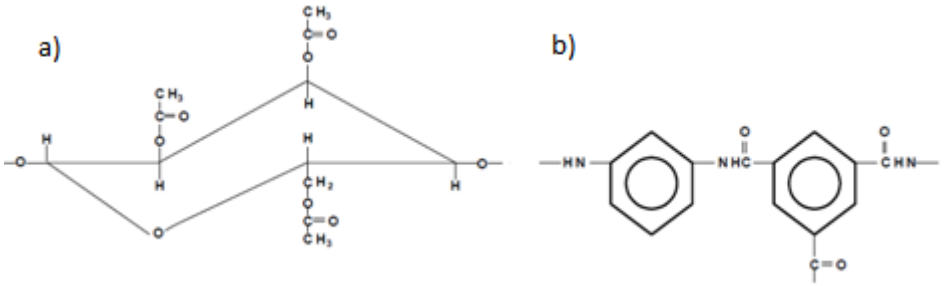

Figure 9 - Chemical structure of polyamide (a) and cellulose triacetate (b) membrane material [28].

Current CA membrane is usually made from a blend of cellulose diacetate and triacetate. The membrane is formed by phase inversion (immersion precipitation) through the casting of a thin film acetone-based solution of cellulose acetate polymer with swelling additives onto a non-woven polyester fabric.

Composite polyamide membranes are manufactured in two distinct steps. First, a polysulfone support, that is very porous (do not have the ability to separate water from dissolved ions), is cast onto a non-woven polyester fabric. Secondly, a semipermeable membrane skin is formed on the polysulfone substracte by interfacial polymerization of monomers containing amine and carboxylic acid chloride functional groups [28].

Polyamide membranes are stable over a wider pH range than cellulose acetate membranes that undergoes hydrolytic decomposition through the substitution of hydroxyl groups for acetyl groups at alkaline pH's [29]. However, polyamide membranes are susceptible to oxidative degradation by free chlorine (chlorination destroy hydrogen bonds in polyamide chains) [30], while cellulose acetate membranes can tolerate limited levels of exposure to free chlorine. Compared to a polyamide membrane, the surface of cellulose acetate membrane is smooth and has little surface charge. Due to the neutral surface and tolerance to free chlorine, cellulose acetate membranes will usually have a more stable performance than polyamide membranes in applications where feed water has a high fouling potential.

RO process drawbacks

However, the water obtained by RO process still being expensive, mainly due to the high energy consumption at RO plants, as well as due to the need of membrane replacements in each 2 - 5 years [2] due to the fouling phenomenon.

Despite chemical suppression usage, RO plants which the percentage of water recovered is around 35 to 50% produce high concentrated brine, which is inevitably discharged back into the sea, causing serious problems in marine environment that is very vulnerable to salinity changes [31] .

Membrane distillation (MD)

Membrane distillation (MD) is another membrane process that is emerging as a viable desalination technology, because of its lower energy requirements.

The driving force of this process is the vapour pressure difference, which is established by a temperature difference across the membrane. The latter in turn is established by placing the hot process solution (seawater) on one side of the membrane, whereas the other side of the membrane is kept cold. The higher vapour pressure of the hot solution causes that water starts to evaporate at the hot side of the membrane; the vapour penetrates though the membrane pores and then condensed on a cold fluid or on a cold surface, depending on the configuration of the cold side of the membrane [32,33]

Compared to conventional distillation, MD requires lower energy consumption and can operate at lower temperatures. Compared to RO, it causes much less fouling and the membranes used do not need to have great mechanical strength or flexibility required in RO process. Additionally, the chemical interaction between feed solution and the membrane is also lower.

However, membranes with the characteristics most suitable for the process are not available yet at reasonable prices [32] and the energy requirements of the process are still high to desalinate water [33,34].

1.7. Forward osmosis process

Osmosis is defined as the movement of water molecules across a semi-permeable due a difference in osmotic pressure across the membrane.

Osmotic pressure is the driving force for many applications in the field of the water treatment and desalination, food processing or power generation [35].

Current desalination technologies are still expensive and energy intensive, the latter is the most significant contributor to the cost of desalination processes. Hence, reduction in energy usage is the main factor to take into account to reduce desalination costs.

Forward (or direct) osmosis (FO) is a process that may be able to desalinate water sources at reduced cost. In FO like RO water is transported across a semi-permeable membrane that retains salts. However, instead of using hydraulic pressure to exceed the osmotic pressure of an aqueous feed solution to create a driving force that promotes water transport through the membrane; the FO process utilizes as driving force an osmotic pressure difference. A “draw” solution having higher osmotic

pressure than the saline feed is placed at the permeate side of the membrane and the water passes through the membrane by osmosis.

The absence of high hydraulic pressure in FO leads to a reduction of the fouling phenomenon [36]; this fouling problem causes a significant increase of operation cost in RO, up to 50% of the total costs [37]. Additionally, the absence of fouling phenomenon can result in the elimination of the seawater pre-treatment stage compulsory in RO desalination. Thus, operation costs will certainly be lower compared to RO. However, FO requires separation of water from the "draw" solution; this can be achieved by several methods such as nanofiltration, multiple columns distillation or electromagnetic separation, depending on solute used to make the "draw" solution and on the energy consumption.

The osmotic pressure of an aqueous solution can also be raised by increasing its temperature or concentration which means that high osmotic pressure gradients can be achieved in FO process leading to high water rate fluxes and recovery. At high recovery from typical seawater, the salt may be induced to precipitate what eliminates the need of brine discharge. RO cannot achieve this high recovery due to pump limitations and membrane housings.

Pressure-retarded osmosis (PRO) is another osmotic pressure driven process that uses the water flux across a selective membrane from, concentrated brine (seawater) to fresh water (river water) to drive turbines in order to produce electricity [35,38]. However, the osmotic pressure difference between seawater and fresh water is about 26 bar and the optimal working pressure for power generation ranges from 11 bar to 15 bar, so a hydraulic pressure is applied in the opposite direction of the osmotic pressure gradient in order to achieve the ideal working pressure gradient.

The general equation to express water transport in FO, RO and PRO is

$$J_w = P\ \sigma\Delta\pi - \Delta P \quad \textbf{Eq. 10}$$

Where J_w is the water flux, P the water permeability constant of the membrane, σ is the reflection coefficient that is determined by the rejection of the membrane and it approaches 1 for total rejection; $\Delta\pi$ is the osmotic pressure difference and ΔP the applied pressure. For RO $\Delta P > \Delta\pi$; For PRO $\Delta P < \Delta\pi$; And for FO ΔP is zero.

The flux directions of water for the three processes are illustrated in Figure 10.

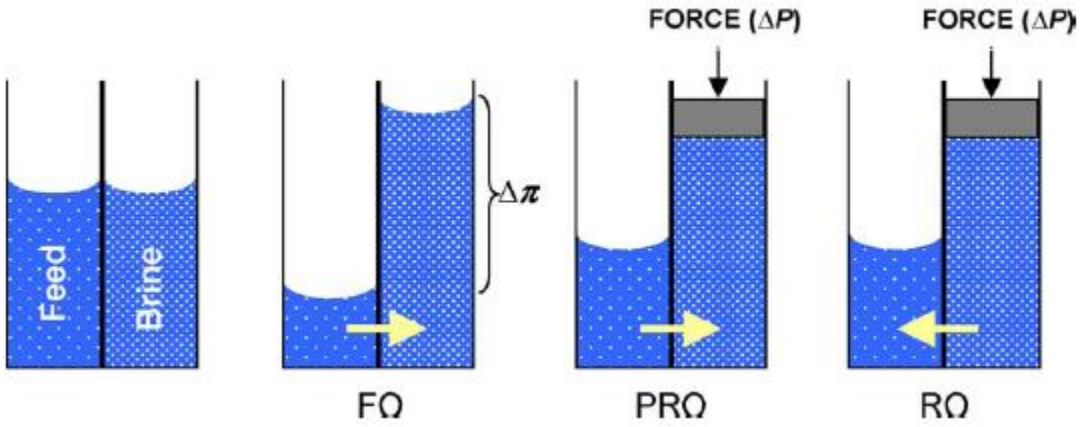

Figure 10- Solvent flows in FO, PRO, and RO [35].

1.7.1. How to choose a draw solution

Draw solution is the solution placed on the permeate side of the membrane that triggers the driving force across the membrane. Thus, the selected draw solution must have higher osmotic pressure than the feed solution.

The ideal FO desalination process should have zero-liquid discharge (ZLD) which requires high water recovery. Additionally, high water recovery is only obtainable at large osmostic driving force. Thus, the ideal draw solute must be able to generate high osmotic pressure at low concentration, meaning it has to be highly soluble in water and have low molecular weight [37].

When the draw solute used is not edible it has to be recovered from draw solution after FO process. Thus, the draw solute must also be economic to remove and reuse. This is the most important criterion since the FO energy consumption is mainly related to the draw solution reconcentration.

Additionally, the draw solute must be chemically inert to the membrane in order to not react or degrade, as well as being non-toxic for humans, since trace amounts may be present in the product water.

Multivalent ions may be preferable since they are also bigger in size which prevent them from diffusing across the membrane decreasing the process driving force and make them easy to separate by nanofiltration [35].

Draw solutes suggested and tested for FO desalination

In 1965 Batchelder [40] described the use of sulphur dioxide (SO_2) (volatile solute) as draw solute for FO and suggested its recovery by heated gas stripping operation in which the heated draw solution would pass in counter-current with warm air in a stripping column. Such operation could be operated at 150F to 190F.

In the same year, Glew [41] described the use of sulphur dioxide and aliphatic alcohols as draw solution and their recovery by distillation.

In 1972 Frank [42] described the use of aluminium sulphate as draw solute which would precipitate into aluminium hydroxide and calcium sulphate from contact with calcium hydroxide after FO. The precipitate could then be easily removed from the draw solution by several methods such as decanting.

In 1970s some authors such as Kessler and Moody [43] or Kravath and Davis [44] also proposed the use of sugars as glucose and fructose as draw solutes for FO in order to produce a nutritious drink. Separation of the draw solute is unnecessary, since the final diluted solution is intended for ingestion.

In 2002 McGinnis [45] suggested a two-stage FO process that relies on the use of draw solutes having high temperature dependence solubilities such as potassium nitrate (KNO_3) and sulphur dioxide (SO_2). In the first stage seawater (pre-heated within the range of 60 to 100 ºC) is subjected to "natural" osmosis from contact with a KNO_3 draw solution along a semi-permeable membrane. The diluted KNO_3 solution is afterwards cooled in a heat exchanger by incoming seawater in order to promote KNO_3 precipitation. In the second stage the diluted KNO_3 solution serves as the feed solution for FO while SO_2 under-pressure solution serves as the draw solution. Water permeation from the feed side dilutes the SO_2 draw solution. The sulphur dioxide is then removed from water by heating and as a result potable water is obtained.

Recently McCutcheon et al. [39, 46, 47] suggested as draw solution a mixture of ammonia and carbon dioxide gases in an aqueous solution due to their high solubility and low molecular weight, which lead to a high osmotic efficiency. Once in aqueous solution this mixture can originate three salts, ammonium bicarbonate (NH_4HCO_3), ammonium carbonate ($(NH_4)_2CO_3$) and ammonium carbamate ($NH_2CO_2NH_4$) which is by far the most soluble of the three salts. For this reason it is desirable to achieve higher concentration of ammonium carbamate relative to the other dissolved species in solution and this can be achieved by increasing the ratio ammonia to carbon dioxide which can produce osmotic pressures in excess of 250 atm.

This draw solute can be easily recovered by heating the diluted draw solution at an appropriate temperature in order to promote the decomposition of the dissolved salts into ammonia and carbon dioxide gases. At atmospheric pressure the decomposition occurs near 60 ºC. The gases can then be removed from the solution by distillation or membrane gas separation.

In this study the authors also compared the energy requirements of different desalination technologies with the using FO followed by single vacuum distillation (FO-LT) to recover the draw solute (Table 3). The percentage of energy reduction for FO-LT desalination was 72% relative to RO desalination and 85% relative to multi-stage flash distillation (MSF).

Table 3- Comparison of energy requirements of current seawater desalination technologies to the ammonia-carbon dioxide FO process [47].

Technology	Electrical energy ($kWh.kgal^{-1}$)	Electrical energy ($kWh.m^{-3}$)	Steam pressure (psia)	Equivalent work ($kWh.m^{-3}$)	Percent energy savings using low temp. FO
MSF	10.04	2.65	25.7	5.66	85.1%
MED-TVC	6.04	1.60	25.7	4.05	79.2%
MED-low temp.	6.04	1.60	6	3.21	73.8%
RO-energy recovery	11.43	3.02	n/a	3.02	72.1%
FO (low tem. 1.5 M feed)	0.92	0.24	1.07	0.84	

Magnetoferritin has also been tested as a potential draw solute [35] which could be rapidly separated from the product water applying a magnetic field.

The osmotic pressures of different possible draw solutions at different concentrations are presented in Figure 11.

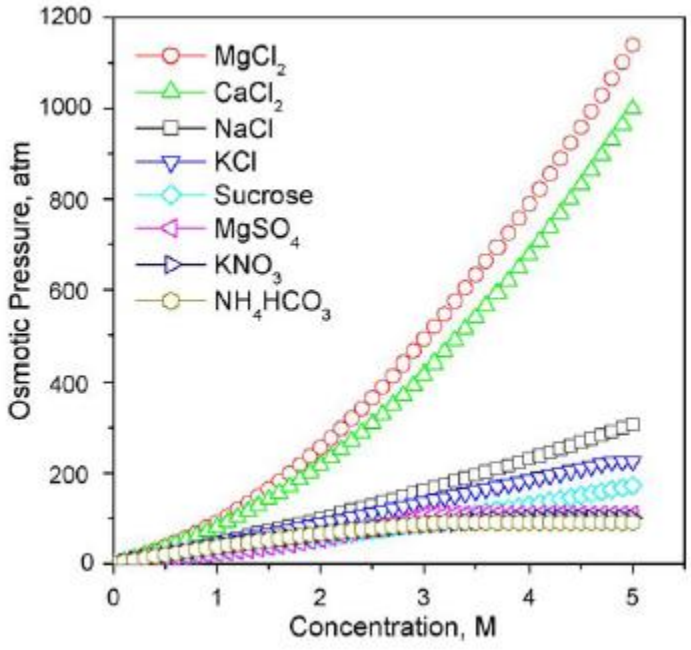

Figure 11- Osmotic pressure as a function of solution concentration at 25ºC for various potential draw solutions [35].

1.7.2. Concentration polarisation in FO

The water flux in osmotic processes is described by Eq.10, where $\Delta\pi$ is the osmotic pressure difference across the membrane. However, in order to determine the experimental water flux several researchers assumed that the effective driving force

was the Δπ of the bulk and as result the water flux obtained was much lower than the one theoretically expected [46,49]. The lower-than-expected flux was explained by the researchers to be caused by concentration polarisation (CP), since due to mass transport resistance the solute's concentration difference across the membrane active layer is lower than the solute concentration difference in the bulk solution. In osmotic-driven processes two types of CP take place, external CP and internal CP [35].

1.7.2.1. External concentration polarisation (ECP)

External concentration polarisation (CP) occurs in FO on both, feed and permeate sides of the membrane.

When the feed flows on the active layer of the membrane and the solutes build up at the active layer due to water permeation, it is called concentrative external CP. This phenomenon is similar to CP in pressure-driven processes. Additionally, in FO the permeating water dilutes the draw solution in contact with the permeate side of the membrane and this phenomenon is called dilutive external CP. Both concentrative and dilutive external CP phenomena reduce the effective osmotic driving force of FO and so the water flux.

External CP effects can be mitigated by increasing flow velocity and turbulence at the membrane surface [35].

In order to evaluate the performance of FO in the absence of ICP (described below), Gordon et al. [50] conducted several FO experiments using the FO membrane provided by HTI. In these experiments the draw solution was placed against the active layer and the feed, DI water, was placed against the support layer. Three solutes of varying molecular weight were used as draw solutes and additionally the hydraulic permeability of the FO membrane used was determined in a crossflow RO configuration. The results are shown in Figure 12.

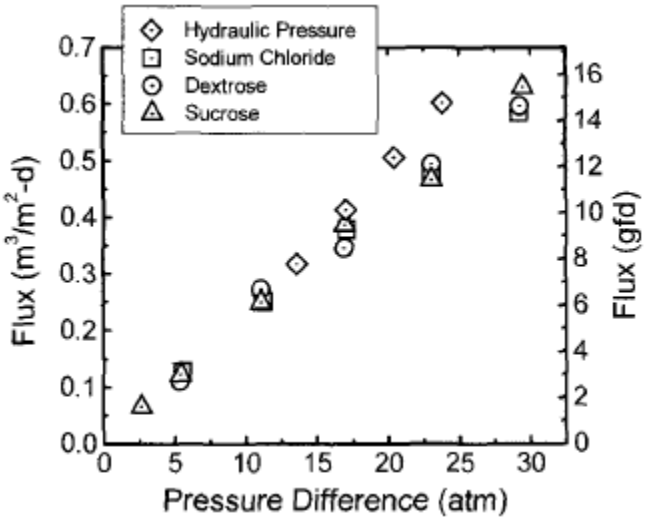

Figure 12-FO water flux as a function of driving force (pressure difference) for different draw solutes. Also presented are data points (open diamonds) for pure water flux against pressure (hydraulic) difference obtained in an RO type experiment with the same membrane [50].

As can be seen flux varies linearly with osmotic pressure difference and the pure water permeability data has practically the same slope as the FO data, what suggest a negligible ECP (dilutive ECP in this case) effect in this process. The milder effects of ECP in FO compared to the effects in pressure-driven processes were also confirmed by McCutcheon et al. [46] and it can be explained by the relatively low water fluxes in FO. Moreover, in the absence of ICP, the molecular weight of the draw solute barely has impact on FO performance.

1.7.2.2. Internal concentration polarisation

Internal concentration polarisation (ICP) occurs within the porous support layer of asymmetric membranes and for this reason it cannot be mitigated by altering hydrodynamic conditions. This phenomenon can promote a reduction in water flux superior to 80% [50, 51, 52] in FO processes.

The non-linear trend observed in Figure 13 [46] is typical of a FO process affected by ICP, the type of concentration polarisation dominant in FO.

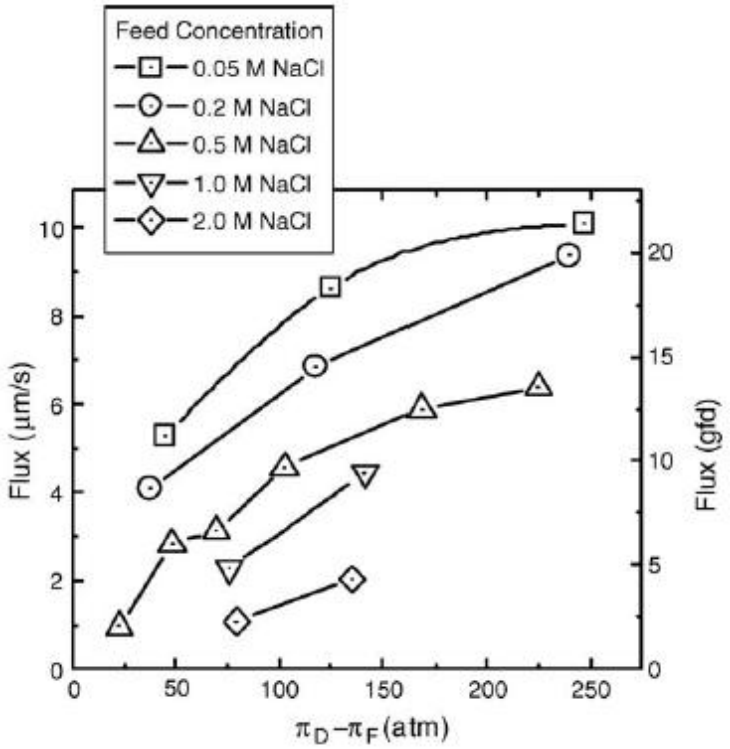

Figure 13- Flux data for a variety of feed solution (NaCl) concentrations. The water flux is presented as a function of the difference in bulk osmotic pressures of the draw and feed solutions [46].

Two types of internal concentration polarisation can arise in FO, depending on membrane orientation. Both types will be described next.

Dilutive ICP

If the membrane active layer is against the feed solution and the porous support against the draw solution, the solute in draw solution must permeate the porous support layer to the interior surface of the active layer. However, as water crosses the active layer into the support layer it promotes the draw solute dilution by convection and this phenomenon is referred as “dilutive ICP” [35].

In the presence of “dilutive ICP” the molecular weight of the draw solute affects water flux in FO, since heavier solutes diffuse slowly through the porous of the support layer and so the dilutive ICP is expected to be more severe. This was confirmed experimentally in [50] and the results are shown in Figure 14.

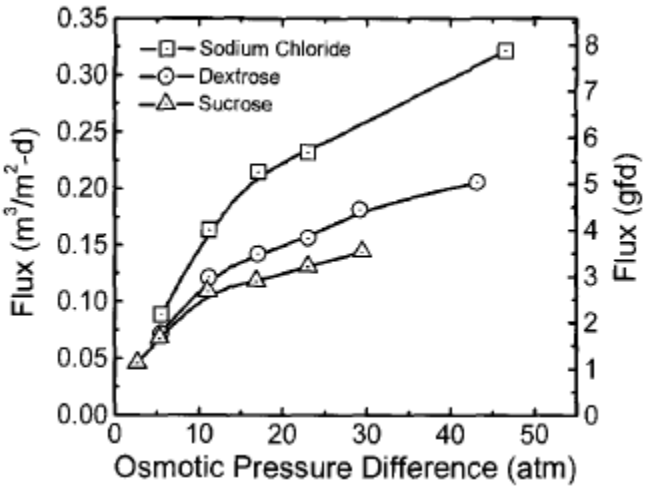

Figure 14-Flux data for a variety of draw solution concentrations [50].

McCuthcheon et al. [46] also proved that in the presence of "dilutive ICP", high concentration of the draw solutions leads to a reduction in membrane performance ratio (shown in Figure 15). This is explained by the increased severity of the "dilutive ICP" due to increased water flux generated by the high concentration of the draw solution.

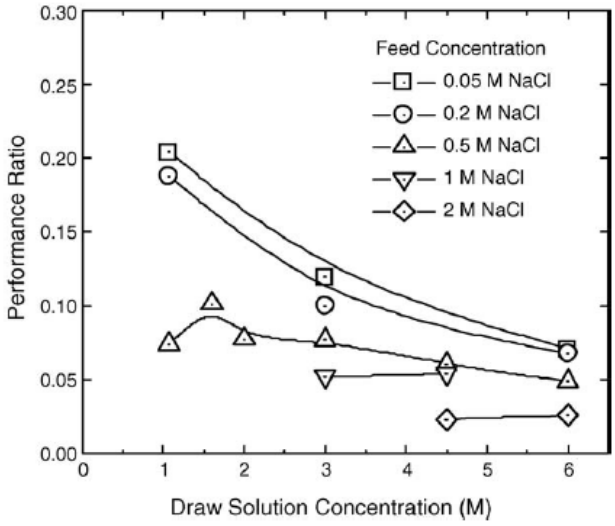

Figure 15- The effect of draw solution concentration on the performance ratio for various feed solution concentrations [46].

Concentrative ICP

On the other hand, when the membrane active layer is placed against the draw solution and the porous support layer against the feed solution, the water permeating from the porous support layer through the active layer causes increased concentration of solutes at the interior surface of the active layer and this phenomenon is referred as "concentrative ICP" [35].

Modelling internal concentration polarisation

Loeb et al. [49] introduced Eq.11 that describes water flux (J_w) in FO without considerate membrane orientation.

$$J_w = \frac{1}{K} ln \frac{\pi_{Hi}}{\pi_{Low}}, where\ K = \frac{t\tau}{\varepsilon D_s} \quad \textbf{Eq. 11}$$

K is the resistance to solute diffusion within the membrane porous support layer, and π_{Hi} and π_{Low} are the osmotic pressures of the bulk draw solution and feed solution, respectively. On the other hand t, τ, and ε are the thickness, tortuosity and porosity of the membrane, while D_s is the diffusion coefficient of the solute. However, it was recently demonstrated that Eq.11 is valid only for very low water fluxes and so more general equations were developed for "concentrative ICP" and "dilutive ICP", respectively:

$$K = \frac{1}{J_w} ln \ \frac{B + P\pi_{Hi} - J_w}{B + P\pi_{Low}} \quad \textbf{Eq. 12}$$

$$K = \frac{1}{J_w} ln \ \frac{B + P\pi_{Hi}}{B + J_w + P\pi_{Low}} \quad \textbf{Eq. 13}$$

Where B is the solute permeability coefficient of the active layer of the membrane, which can be determined from an RO-type experiment using Eq.14 and P is the membrane permeability (presented in Eq.10)

$$B = \frac{1 - R \ \ P(\Delta P - \Delta\pi)}{R} \quad \textbf{Eq. 14}$$

Data collected from forward osmosis tests conducted by McCutcheon et al. [52] successfully matched the model described above.

Difference between "dilutive ICP" and "concentrative ICP": role of membrane orientation

Gordon et al. [50] carried out a set of FO experiments in order to study the impact of the "dilutive ICP" and the "concentrative ICP". They used 0.5 M NaCl as a draw solution and concentrations ranging from DI water to 0.375 M NaCl as feed solutions. Then, in one set of experiments the active layer faces the draw solution ("concentrative ICP" takes place) and in the other the active layer faces feed solution ("dilutive ICP" takes place). The results are shown in Figure 16.

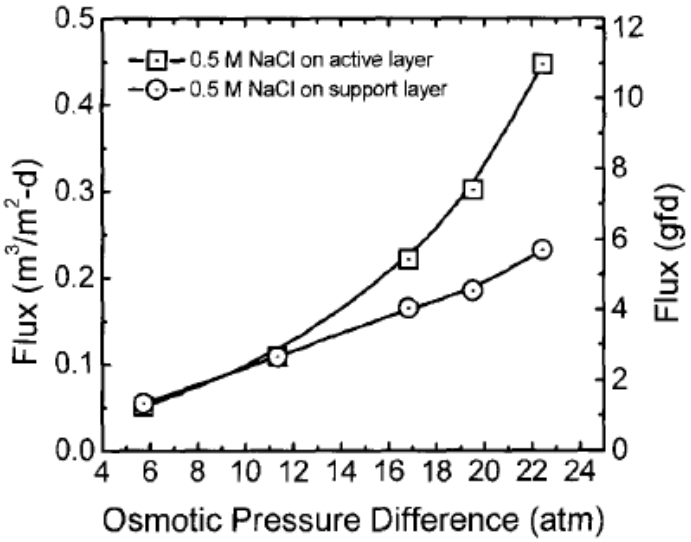

Figure 16- Water flux data for 0.5 M NaCl draw solution and a variety of NaCl feed solutions ranging from DI water to 0.375 M. In one set of experiments (open squares) the 0.5 M draw solution is placed against the active layer of the membrane while in another set of experiments is placed (open circles) is placed against the support layer of the membrane [50].

This study clearly proved that membrane orientation plays an important role in water flux in FO. Experimental data suggests that "concentrative ICP" has lower impact in water flux in FO for NaCl feed/NaCl draw system for higher osmotic pressure differences. However, this assumption cannot be generalized for all feed/draw solutions system, since the effect of ICP depends, among other parameters related to the membrane, on solute diffusivity.

1.7.3. Membranes for FO desalination

At the moment most available membranes to use in FO process are dense semi-permeable membranes which are obtained from RO industry except the commercialized FO membrane developed by Hydration Technologies Inc. (HTI). However, all the FO studies involving RO membranes showed much lower flux than expected [35, 39].

RO membranes typically consist of a very thin surface layer (less than 1 µm), a thick microporous support layer that provides support to the membrane and a thick fabric backing that gives mechanical strength and resistance to tearing of the membrane since RO occurs at extremely high pressures.

However, in FO process membranes are not subjected to high hydraulic pressures which eliminates the need for a thick support layer and the tick fabric backing that can contribute to the development of internal concentration polarisation, that in turn reduce the effective driving force and thus the water flux through the membrane

McCutcheon et al. [39] tested two commercially available flat sheet RO membranes and the commercially available FO membrane (thought to be made of cellulose

triacetate (CTA)) in FO desalination using ammonium bicarbonate (NH_3HCO_3) aqueous solution as the draw (Figure 17). The RO membranes were denoted by the manufacturer as AG (thin film composite membrane of polyamide on a polysulfone backing) and CE (cellulose acetate asymmetric membrane). Secondly, the water permeability of these membranes was determined using a hydraulically pressurized RO crossflow filtration cell (Figure 18).

Results for FO experiment showed much higher flux for CTA membrane than for AG and CE membranes. However in the water permeability test CTA is the membrane showing the lowest flux, which means that membrane permeability, cannot explain the flux difference in FO. Consequently, the flux difference must be explained by the membrane structure.

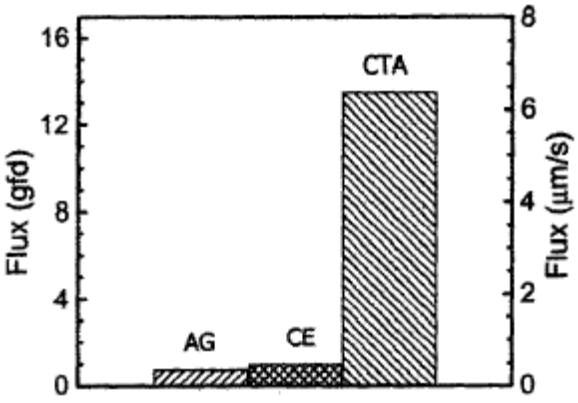

Figure 17- Comparison of water flux in FO mode for the three membranes tested: AG and CE (RO membranes), and CTA (FO membrane). Experimental conditions: 6 M ammonium bicarbonate draw solution, o.5 M sodium chloride feed solution, and temperature of both feed and draw solutions of 50°C [39].

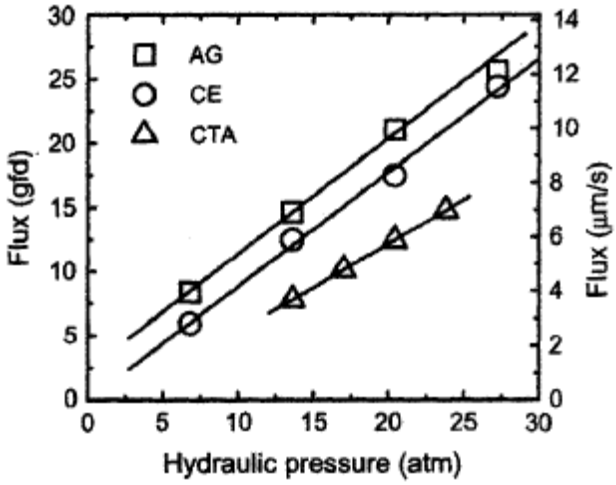

Figure 18- Pure water flux vs. hydraulic pressure for the three membranes tested: AG, CE and CTA [39].

The RO membranes tested in this study, AG (Figure 19 (b)) and CE have both an overall thickness of 140 µm (approximately 50 µm of polymer(s) layer and 90 µm of fabric support layer), while the FO membrane (CTA) shows an overall thickness less than 50 µm and consists of polyester mesh embedded between two layers of cellulose triacetate polymer (Figure 19 (a)).

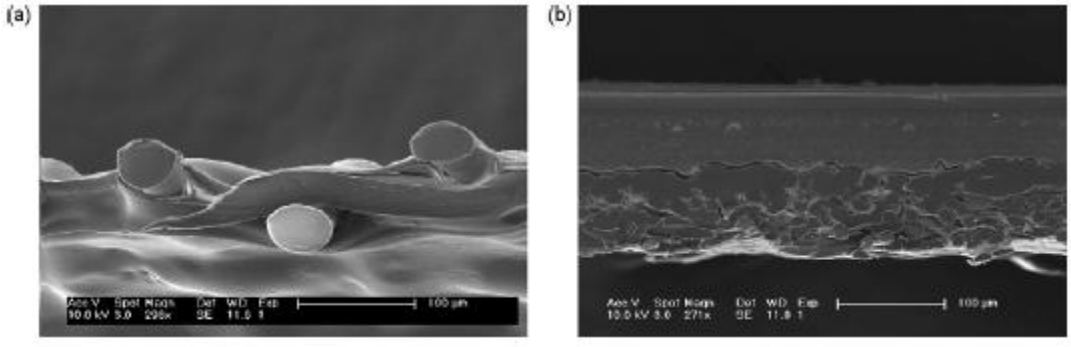

Figure 19- SEM images of both membranes tested in FO process [53]: (a) cellulosic (CTA) membrane. (b) the thin-film composite RO membrane (AG).

The authors of this study concluded that the two major contributing factors for the better performance of CTA in FO may be its thinness and its lack of a thick fabric support.

Recently, based on the factors above some researchers have tried to develop better membranes to apply in FO process. The performance of the membranes developed so far is shown in the table below.

Table 4- Resume of the performance in FO process of the FO membranes so far fabricated.

Membrane	Pure water permeability ($L.m^{-2}.h^{-1}.bar^{-1}$)	%Na Rejection	Reference
CTA, commercialized by HTI (flatsheet)	2.0	>95%	**[46]**
Thin film composite (TFC) membrane composed of Polyamide on Polyethersulfone (PES) support (Hollow fibers)	3.5	≈ 90%	**[54]**
PBI crossilinked by p-xylylene dichloride for 9 hours(Hollow fibers)	1.25	≈ 60%	**[16,55]**

1.7.3.1. Potentiality of Polyimide as a membrane for FO

Polyimide (PI) has been widely used in gas separation, pervaporation **[56]** and liquid filtration, due to its inherently greater chemical, biological and thermal stability as well as its excellent mechanical **[4]**. Recently and for the same reasons PI has also drawn much attention in organic solvent nanofiltration (OSN) technology **[8,57]**. Additionally Wang et al. **[58]** claimed that PI exhibits high selectivity and thin film formability and this make PI a good candidate for a FO membrane. For these reasons polyimide (Lenzing P84), shown bellow, was the polymer studied in this project.

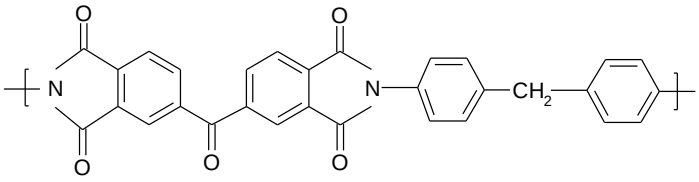

BTDA-MDI 20 % mol

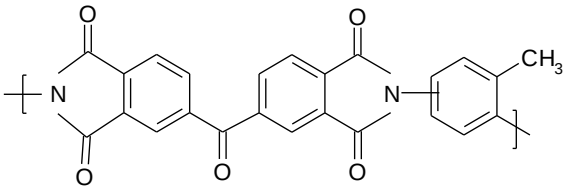

BTDA-TDI 80 % mol

Lenzing P84 is a co-polyimide of 3,3'4,4'-benzophenone tetracarboxylic dianhydride (BTDA) and 20 mol % 4,4'-methylenebis (phenyl isocyanate) (MDI), and 80 mol % 2-methyl-m-phenylene diisocyanate (TDI). There are two isomers of TDI: 2,4-TDI and 2,6-TDI. Lenzing P84 contains 64 mol % 2,4-TDI and 16 mol % 2,6-TDI [56].

2. Implications of literature review and research motivation

As it has been mentioned before, forward osmosis has drawn the attention of the scientific community as new desalination process due to its potential advantages, such as lower energy consumption, higher feed water recovery and reduced fouling. However, with the current FO technology these potential advantages have not been yet reached (Figure 20).

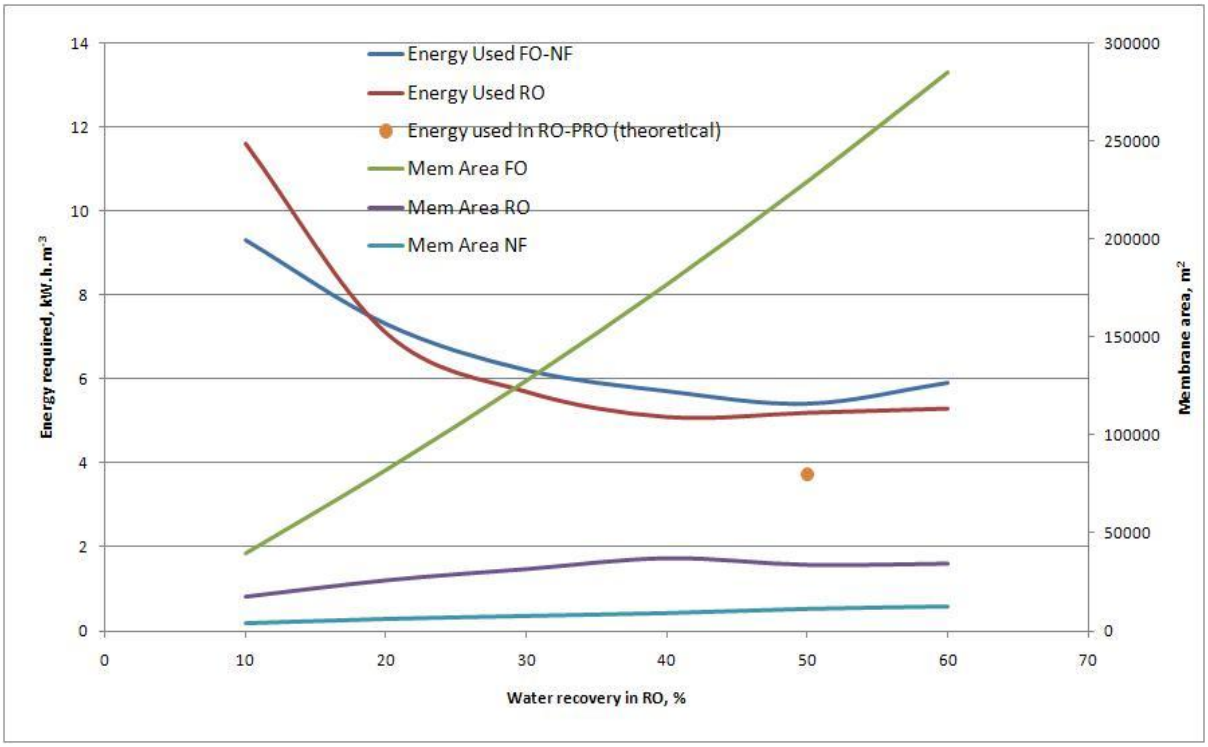

Figure 20- Current energy and membrane area requirements for FO-NF and RO and energy used in RO-PRO theoretically.

In order to achieve these potential benefits and develop FO process as a powerful mean to desalinate water, the membrane performance must be enhanced in terms of permeability and selectivity as well as internal concentration polarisation (ICP) effect, the biggest problem of FO process. Additionally, the development of a draw solute able to generate high osmotic pressure and requiring low energy to be reconcentrated is equally crucial.

The concentration polarisation can be minimized reducing K, the resistance to solute diffusion given in Eq.11 bellow.

$$K = \frac{t\tau}{\varepsilon D_S} \quad \textbf{Eq. 11}$$

Following Eq.11, K can be minimized either by tailoring the membrane structure, such as thickness, tortuosity and porosity, or increasing the diffusion coefficient of the solute (D_s).

Increase D is only possible by increasing the process temperature or by choosing a draw solute with higher diffusivity. However, the choice of the draw solute must be mainly related with its reconcentration method, which must be rather economic. Increasing temperature leads to higher flux as well as higher energy consumption. Therefore, these two factors must be weighed to decide the optimal operating temperature.

On the other hand, reduce K by tailoring the membrane structure can be achieved by decreasing membrane thickness and tortuosity and simultaneously, increasing its porosity. However, tailor membrane tortuosity is more difficult than tailor its thickness and porosity.

This project was focused on the development of a FO membrane combining high permeability with high selectivity. This was accomplished by tailoring the membrane thickness and porosity.

3. Experimental

3.1. Chemicals

Lenzing P84 polyimide powder was purchased from HP polymer GmbH. Sodium chloride, magnesium sulphate, glucose, saccharose, raffinose, α-cyclodextrine, valeric acid, glycerol, 1,6-Hexanediamine (HDA) and polyvinyl pyrrolidone (PVP) were all purchased from Sigma Aldrich. Isopropanol (IPA) was purchased from VWR internacional. Polyethylene glycol (MW 400 $g.mol^{-1}$) (PEG) was purchased from Merck. Dimethylformamide (DMF) and 1,4-Dioxane were purchased from Rathburn Chemicals Ltd. All chemicals were used as received.

3.2. Flat sheet membranes preparation by phase inversion

Nylon fabric (purchased from SEFAR Ltd) with a thickness of 50 µm and porosity of 19% was used as backing to cast membranes, and was pasted to the glass plate using 10 wt.% polyvinyl pyrrolidone (PVP) solution in water. Dope solutions of P84 polyimide were prepared by dissolving varied polymer concentrations in different rations of DMF (solvent) and 1,4 – Dioxane (co-solvent). These mixtures were then continuously agitated overnight to obtain homogeneous dope solutions. Finally, the homogeneous dope solutions were left to disengage air bubbles before membrane casting for further 24 hours. The obtained dope solutions were subsequently used to cast 100 µm thick viscous films on backing using an adjustable casting knife (Elcometer 3700). The casted polymer films were then immersed into a water coagulation bath at room temperature for 1 hour, where phase inversion took place. The resulting membranes were either stored in water, or immersed in aqueous solutions of polyethylene glycol and glycerol (40 and 50 wt.%, respectively) for 12 h and then air dried. The membranes to be crosslinked were transferred from water to the crosslinking solution (HDA in isopropanol). Fallowing this, the membranes were stored in isopropanol to remove residual HDA.

3.3. Chemical analysis

Concentrations of salt solutions were analysed using Inductively Coupled Plasma Mass Spectrometry (ICP-MS) for determining the concentration of Na and Mg. Concentrations of glucose, sacharose, raffinose and α-cyclodextrine were determined using an Shimadzu HPLC system. Valeric acid concentrations were determined using the Shimadzu HPLC with a UV/vis detector set at a wavelength of 210 nm. Separation was accomplished using a CTO – 10AC column. The mobile phase used was DI water, flow rate was set at 0.4 $ml.s^{-1}$and temperature was 35 ºC.

3.4. Dope solution characterization

3.4.1. Viscosity test

Viscosities of dope solutions were measured using a Cannon Instrument Company (Model 2020) viscometer at 20^0C at several rotational speeds of the spindle.

3.4.2. Ternary phase diagram

In order to obtain a ternary phase diagram, dope solutions of 16 wt.%, 18 wt.% and 22 wt.% of P84 were prepared at different DMF/Dioxane ratios. Each solution was

then continuously stirred while the non-solvent (water) was added drop by drop by means of a syringe until non-homogeneity (turbidity) was observed. The total amount of non-solvent added was determined by difference of weights before and after the experiment.

3.5. Membrane characterization

Porous membranes are usually characterized in terms of performance, by the flux and the molecular weight cut-off (MWCO - that is the molecular weight at which the membrane rejects 90%) and in terms of morphology by pore size, surface layer thickness, porosity, etc.

3.5.1. Membrane performance in FO

All the FO experiments were conducted at room temperature, using 35 $g.L^{-1}$ NaCl solution (osmotic pressure of 24.3 bar) as feed and 150 $g.L^{-1}$ MgSO4 solution (osmotic pressure of 37.1 bar) as “draw” solution. Solution containers were placed over balances and the flow was circulated at a rate of 6.5 – 7 $L.h^{-1}$ by means of gear pumps. Membranes coupons with an area of 0.0044 m^2 were cut and placed in a cell (made at imperial workshops). All the experiments were conducted at room temperature with the draw solution facing the active side of the membrane. The step-up used is illustrated in Figure 21.

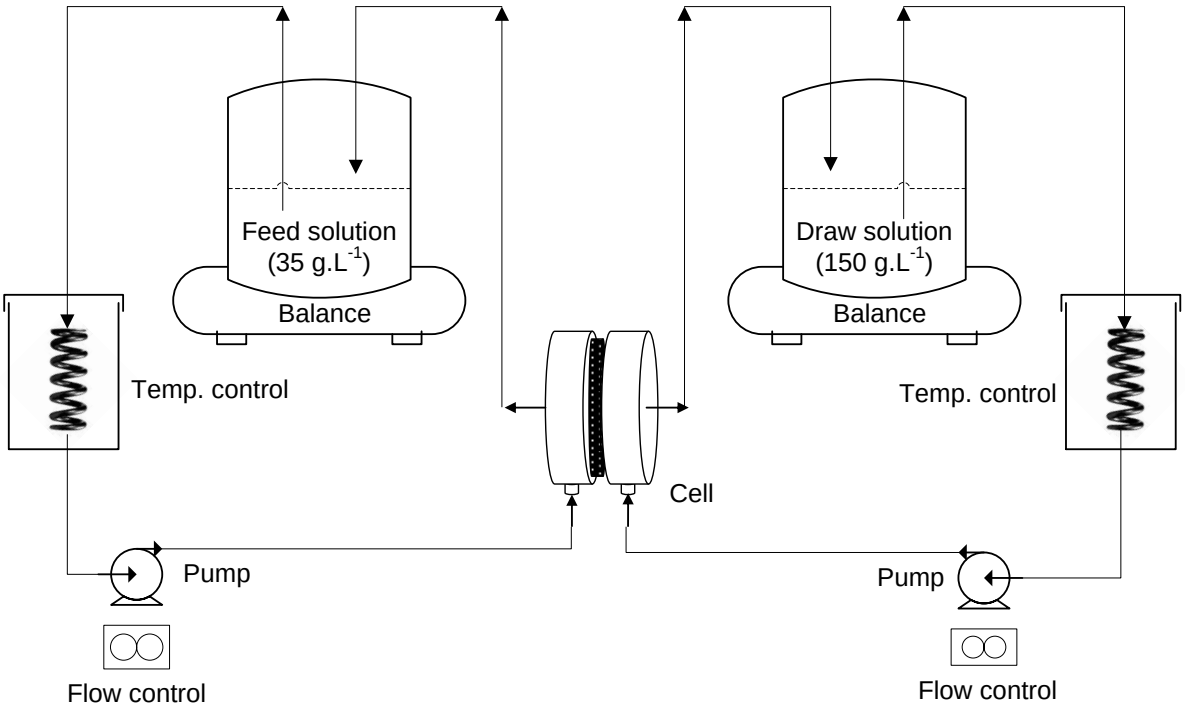

Figure 21- Schematic of experimental FO system used to test membranes in FO process.

Water flux (J_w) was determined by measuring of the weight variation in the draw solution ($\Delta Weight$) per unit of time and per unit of membrane area (A), according to the following equation.

$$J_w = \frac{\Delta Weight}{A.time} \quad \textbf{Eq. 15}$$

The rejection (R) was calculated by the following equation:

$$\%R = \left(1 - \frac{C_p}{C_F}\right) \times 100 \quad \textbf{Eq. 6}$$

Where C_p is the concentration of Na and Mg in draw and feed solutions, respectively after FO run and C_f is the concentration of Na and Mg in feed and draw solution, respectively before FO run.

3.5.2. Nanofiltration experiments

Nanofiltration tests were carried out in order to determine membranes pure water permeability as well as their MWCO. In NF tests feed solutions are forced through the membrane by an applied pressure and the test ends when 50% of the feed has been collected. The NF membrane testing set-up (Sepa ST – Osmonics CA, USA) used is shown in Figure 22.

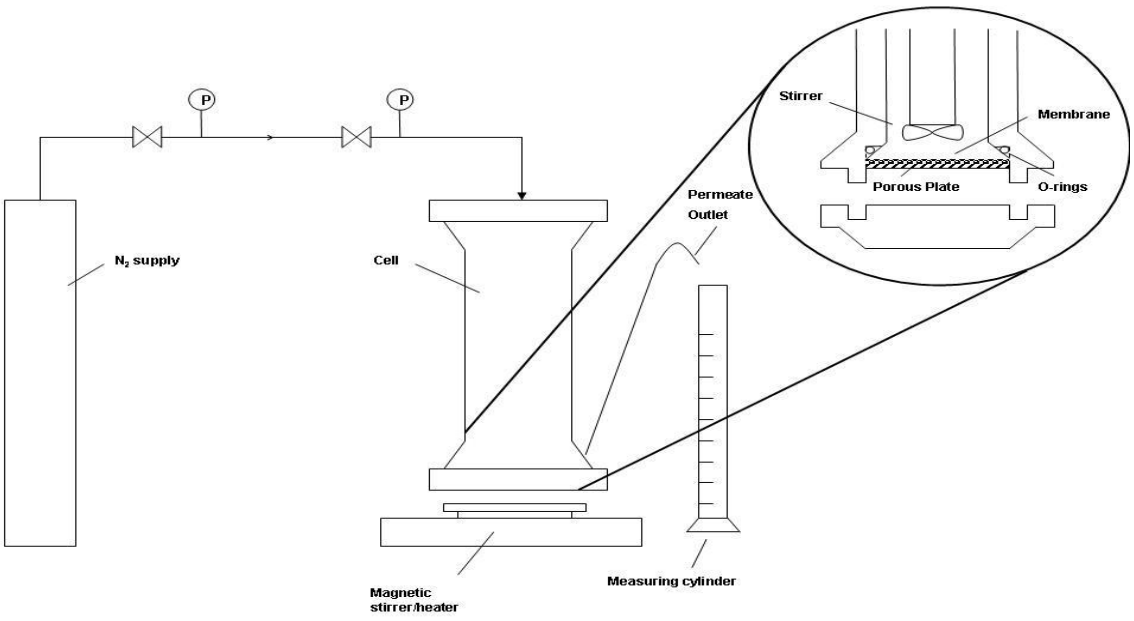

Figure 22- Schematic of experimental pressure cell used to test membranes in nanofiltration process.

Flat sheet membranes were firstly subjected to measure the pure water permeability at 10 bar in the NF set-up (Figure 22). Subsequently, to determine the MWCO curves of the membranes, these were subjected to individually filtrations of 1g.L^{-1} aqueous solutions of valeric acid, glucose, saccharose, raffinose and α-cyclodextrine also at 10 bar. The membranes area used was 0.0019 m^2. In all the experiments membranes active layer were placed against the feed solutions and nitrogen was used to pressurize the system.

The pure water permeability was determined by measuring the volume of permeate (V) per unit of membrane area (A) per unit of time (t) per unit of pressure applied (ΔP), according to the fallowing equation:

$$Permeability = \frac{V}{A.t.\Delta P} \quad \textbf{Eq. 16}$$

The solutes rejection was calculated by Eq.17, where C_p and C_r are the concentrations on permeate and retentate, respectively.

$$\%R = 1 - \frac{C_p}{C_r} \quad \textbf{Eq. 17}$$

MWCO was determined by plotting the rejection (calculated by Eq.17) against the molecular weight for the range of test compounds and determining the molecular weight at which the rejection is 90%.

Table 5- Molecular weight of the solutes used to conduct NF experiments.

Solutes	Molecular weight (g.mol^{-1})
Valeric acid	102.13
Glucose	180.16
Sacharose	342.30
Raffinose	504.42
α-Cyclodextrine	972.84

The mean pore size and pore size distribution were determined according to solute transport model described in section 1.1.3. Following the model, the relationship between solute Stoke radius (r_s) and solute molecular weight (MW) was calculated according to Eq. 9 and the membrane pore size distribution was expressed by the probability density function given in Eq.8, where d_p is the pore size, μ_p is the mean pore size and σ_p the standard deviation.

$$logr_s = -1.4962 + 0.4657\ logMW \quad \textbf{Eq. 9}$$

Table 6- Molecular weight and Einstein-Stoke radius of the solutes used to conduct NF experiments.

Solute	MW (g.mol^{-1})	rs (nm)
Valeric Acid	102.13	0.2751
Glucose	180.16	0.3583
saccharose	342.3	0.4831
Raffinose	504.42	0.5787
α-Cyclodextrine	972.84	0.7858

$$\frac{df(d_p)}{dd_p} = \frac{1}{d_p ln\sigma_p \sqrt{2\pi}} exp\ -\frac{(lnd_p - ln\mu_p)^2}{2(ln\sigma_p)^2} \quad \textbf{Eq. 8}$$

3.5.3. Scanning electron microscopy (SEM)

SEM (Leo 1525 field emission scanning electron microscope, FESEM) was used to take pictures of cross-sectional areas, back and top surfaces of the tested membranes. Samples were mounted onto SEM stubs, and coated with chromium using a chromium sputter coater (Emitech K575X). Applied SEM conditions were: a 7 mm working distance, in lens detector with an excitation voltage of 5kV.

4. Results and discussion

4.1. Effect of polymer concentration on membrane performance

The objective of this section was to study the effect of polymer concentration on membrane performance in FO process. Therefore, membranes were prepared at different polymer concentrations for a fixed solvent system. The fabricated membranes were then tested in FO process and evaluated in terms of flux and rejection. Additionally, membranes were characterized through nanofiltration in terms of MWCO, mean pore size and pore size distribution. Finally, SEM pictures of the fabricated membranes were recorded to observe their morphology.

4.1.1. FO experiments

Membranes with polymer concentrations varying from 14 wt.% to 22 wt.% P84 were casted using only DMF, DMF:Dioxane, 1:3 and DMF:Dioxane, 1:6. The fabricated membranes were tested in FO process and the results will be presented and discussed bellow.

Solvent system consisting only of DMF

Table 7- Effect of polymer concentration on P84 membranes prepared only with DMF.

Membrane composition		Flux ($kg.m^{-2}.h^{-1}$)
P84, wt.%	16%	7.78
DMF, wt.%	84%	
P84, wt.%	18%	25.85
DMF, wt.%	82%	
P84, wt.%	22%	0.507
DMF, wt.%	78%	

The results showed that when P84 dope solutions containing only DMF as solvent are used to cast membranes, the water flux in FO process flows from the $MgSO_4$ solution to NaCl solution (Table 7).The water flux observed can only be explained by the elevation of the osmotic pressure on the feed side of the membrane. It has been shown in section 1.4.4 that P84 dope solutions containing high DMF contents result in porous membranes showing finger like structures (macrovoids). This open structure may be facilitating the NaCl (that is smaller than $MgSO_4$) buildup and thus causing the increased osmotic pressure on the feed side of the membrane. However, further tests need to be done to confirm this theory.

DMF:Dioxane - 1:3

Table 8- Effect of polymer concentration on P84 membranes prepared with a solvent system consisting of DMF:Dioxane, 1:3.

Membrane composition		Flux ($kg.m^{-2}.h^{-1}$)	Permeability ($kg.m^{-2}.bar.h^{-1}$)	% R (Na)	% R (Mg)
P84 wt.% DMF:Dioxane	14% 1:3	2.96	0.231	87.2%	97.9%
P84 wt.% DMF:Dioxane	16% 1:3	2.93	0.229	87.9%	98.0%
P84 wt.% DMF:Dioxane	18% 1:3	3.37	0.264	89.7%	99.1%
P84 wt.% DMF:Dioxane	22% 1:3	3.31	0.259	89.4%	98.5%

*All experiments were done at least twice and the results shown are an average of the results obtained in each experiment.

Table 8 shows the performance of the 14 wt%, 16 wt.%, 18 wt.% and 22 wt.% P84 membranes casted with DMF:Dioxane, 1:3 ratio in FO process. The results show that the polymer concentration does not play an important role for this solvent system, since the membranes water permeability and salts rejection is approximately the same.

DMF:Dioxane, 1:6

Table 9 - Effect of polymer concentration on P84 membranes prepared with a solvent system consisting of DMF:Dioxane, 1:6.

Membrane composition		Flux ($kg.m^{-2}.h^{-1}$)	Permeability ($kg.m^{-2}.bar.h^{-1}$)	% R (Na)	% R (Mg)
P84 wt.% DMF:Dioxane	14% 1:6	4.35	0.340	84.8%	95.8%
PI(w/w) DMF:Dioxane	16% 1:6	5.07	0.396	85.3%	97.6%
P84 wt.% DMF:Dioxane	18% 1:6	5.95	0.465	87.0%	98.9%
P84 wt.% DMF:Dioxane	20% 1:6	3.26	0.255	92.0%	99.4%

*All experiments were done at least twice and the results shown are an average of the results obtained in each experiment.

Table 9 shows the performance of the 14 wt%, 16 wt.%, 18 wt.% and 20 wt.% P84 membranes casted with DMF:Dioxane, 1:6 ratio in FO process. In this solvent system dope solutions show higher viscosities in comparison to DMF:Dioxane, 1:3 system. These viscosities seem to be significantly high to delay the liquid-liquid demixing, since the results showed an elevation in salts rejection with the increase of the polymer concentration, which means that membranes are becoming denser. Additionally, increasing polymer concentration from 14 wt.% to 18 wt.% also promotes water flux enhancement. However, the increase of polymer concentration from 18 wt.% to 20 wt.% leads to a great densification of the resulting membrane, resulting in the flux reduction.

4.1.2. Nanofiltration experiments

Membranes casted with polymer concentrations of 16 wt.%, 18 wt.% and 20 wt.% with DMF:Dioxane, 1:6 were subjected to individually filtrations of aqueous solutions of valeric acid, glucose, sacharose, raffinose and α-cyclodextrine in order to determine membranes MWCO, pore size and pore size distribution. The results will be presented and discussed next.

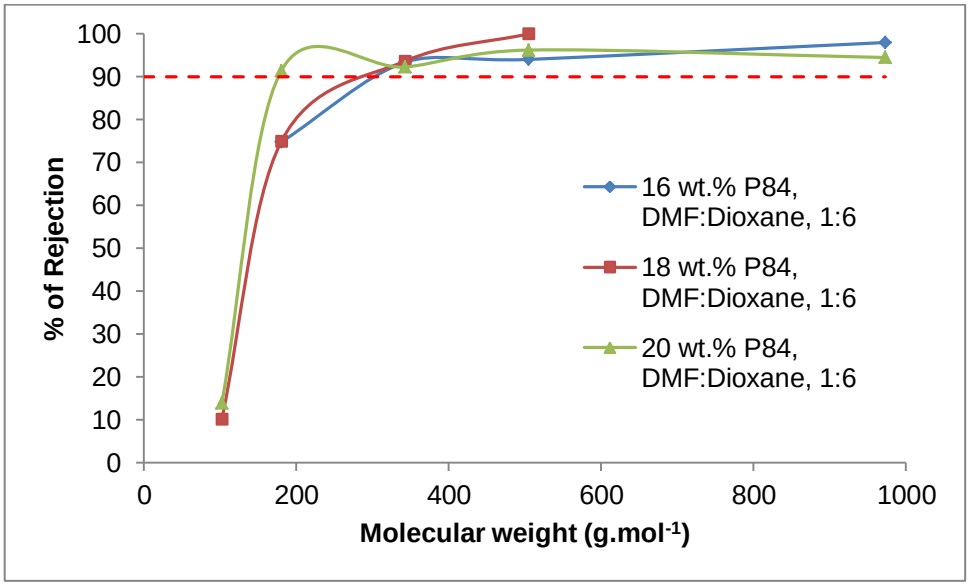

Figure 23- Rejection performance of the membranes 16, 18 and 20 wt.% P84 prepared with DMF:Dioxane, 1:6.

Table 10- MWCO of 16, 18 and 20 wt.% P84 prepared with DMF:Dioxane, 1:6.

Membrane composition	MWCO
16 wt.%, DMF:Dioxane - 1:6	312.9
18 wt.%, DMF:Dioxane - 1:6	310.8
20 wt.%, DMF:Dioxane - 1:6	178.7

Once again, is shown (table 10) that the effect of increasing the concentration of P84 from 16 wt.% to 18 wt.% is practically negligible. The MWCO curves of the respective membranes are pretty similar as well as their MWCO (312.9 and 310.8 $g.mol^{-1}$). However, the slight increase of the polymer concentration from 18 wt.% to 20 wt.% leads to a great densification of the resulting membrane. This can be observed in its MWCO – 178.7 $g.mol^{-1}$, that is about half of the MWCO of 16 wt.% and 18 wt.% membranes.

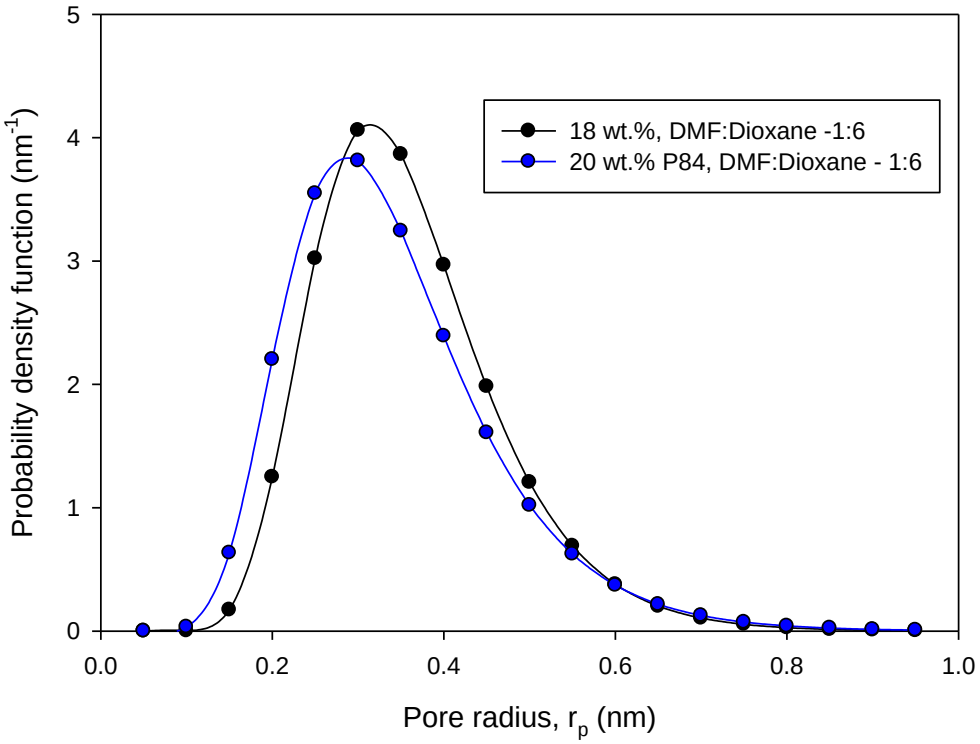

Figure 24- Pore size distribution probability density curves of membranes 18 and 20 wt.% P84 prepared with DMF:Dioxane 1:6.

Figure 24 shows the pore size distribution of the membranes 18 and 20 wt.% P84, DMF:Dioxane, 1:6. Both curves represented show similar pore size distribution. However, 20 wt.% P84 is moving towards left, which indicates reduced mean pore size. This in turn explains 20 wt.% P84 low MWCO and poor performance in terms of flux in FO process, compared to 18 wt.% P84.

4.2. Effect of solvent/co-solvent ratio on membrane performance

As it was already mentioned, the ratio of solvent/co-solvent in the casting solution has great impact in membrane morphology. The addition of co-solvent (that is a non-solvent to the polymer) to the casting solution promotes the entanglement of the polymer chains, which elevates membrane porosity and simultaneously reduces membrane pore size. Therefore, it is crucial to determine the perfect solvent/co-solvent ratio for a given polymer.

The solvent system studied was DMF:Dioxane, which is the most commonly solvent system used to prepare polyimide P84 membranes. In this system, DMF is the polymer solvent, whereas dioxane is the polymer co-solvent that is added to the casting solution.

In this section, the effect of solvent/co-solvent ratio on membrane performance and morphology was studied by preparing membranes with a certain concentration of polymer at different ratios of solvent/co-solvent. To better understand membranes

performance in FO process, membranes morphology was once more studied through nanofiltration experiments and SEM pictures.

4.2.1. FO process

The membranes casted at different solvent/co-solvent ratios were then tested in FO process and their performance was evaluated in terms of flux and rejection. The results will be presented and discussed next.

14 and 16 wt.% P84

Table 11-Effect of solvent/co-solvent ratio on 14 wt.% P84 membrane.

Membrane composition	Flux ($kg.m^{-2}.h^{-1}$)	Permeability ($kg.m^{-2}.bar^{-1}.h^{-1}$)	% R (Na)	% R (Mg)
P84 wt.% 14% DMF:Dioxane 1:3	3.06	0.231	87.2%	97.9%
P84 wt.% 14% DMF:Dioxane 1:6	4.35	0.340	84.8%	95.8%

*All experiments were done at least twice and the results shown are an average of the results obtained in each experiment.

Table 12-Effect of solvent/co-solvent ratio on 16 wt.% P84 membrane.

Membrane composition	Flux ($kg.m^{-2}.h^{-1}$)	Permeability ($kg.m^{-2}.bar^{-1}.h^{-1}$)	% R (Na)	% R (Mg)
P84 wt.% 16% DMF:Dioxane 1:3	2.93	0.229	87.9%	98.0%
P84 wt.% 16% DMF:Dioxane 1:6	5.07	0.396	85.3%	97.6%

*All experiments were done at least twice and the results shown are an average of the results obtained in each experiment.

From tables 11 and 12 can be observed an improvement in water flux when the dioxane content in the dope solution increases to double. However, due to their low polymer concentration, the salt rejection of these membranes is still low compared to what is required for FO process. Therefore, higher polymer concentrations were tried afterwards.

18 wt.% P84

Table 13-Effect of solvent/co-solvent ratio on 18 wt.% P84 membrane.

Membrane composition	Flux ($kg.m^{-2}.h^{-1}$)	Permeability ($kg.m^{-2}.bar^{-1}.h^{-1}$)	% R (Na)	% R (Mg)
P84 wt.% 18% DMF:Dioxane 1:3	3.37	0.264	89.7%	99.1%
P84 wt.% 18% DMF:Dioxane 1:6	5.95	0.465	87.1%	98.3%
P84 wt.% 18% DMF:Dioxane 1:8	2.90	0.226	92.0%	97.7%

*All experiments were done at least twice and the results shown are an average of the results obtained in each experiment.

In 18 wt. % P84, the increase in solvent/co-solvent ratio from 1:3 to 1:6 has led to a big increase in flux, while the rejection remains almost constant. This means that the membrane porosity was improved. However, when the solvent/co-solvent ratio changed from 1:6 to 1:8, the water flux dropped and the salt rejection improved. At 1:8 ratio, the entanglement of the polymer chains during phase inversion is so high that a dense membrane is obtained.

22 wt.% P84

Table 14-Effect of solvent/co-solvent ratio on 22 wt.% P84 membrane.

Membrane composition	Flux ($kg.m^{-2}.h^{-1}$)	Permeability ($kg.m^{-2}.bar^{-1}.h^{-1}$)	% R (Na)	% R (Mg)
P84 wt.% 22% DMF:Dioxane 1:1	1.48	0.116	92.8%	98.9%
P84 wt.% 22% DMF:Dioxane 1:3	3.31	0.259	89.4%	98.5%
P84 wt.% 22% DMF:Dioxane 1:5	1.81	0.141	96.0%	99.4%

*All experiments were done at least twice and the results shown are an average of the results obtained in each experiment.

For 22 wt.% P84 a similar situation is observed. The increase in DMF:Dioxane ratio from 1:1 to 1:3 led to an improvement in flux, while the rejection remains practically constant. This suggests that membrane porosity was improved. On the other hand, the increase in ratio from 1:3 to 1:5 led to membrane densification, since the flux dropped and the rejection improved.

4.2.2. Nanofiltration experiments

Membranes casted with polymer concentrations of 18 wt.% with DMF: Dioxane ratios of 1:3, 1:6 and 1:8 were subjected to individually filtrations of aqueous solutions of valeric acid, glucose, sacharose, raffinose and α- cyclodextrine in order to determine membranes MWCO, pore size and pore size distribution. The results will be presented and discussed next.

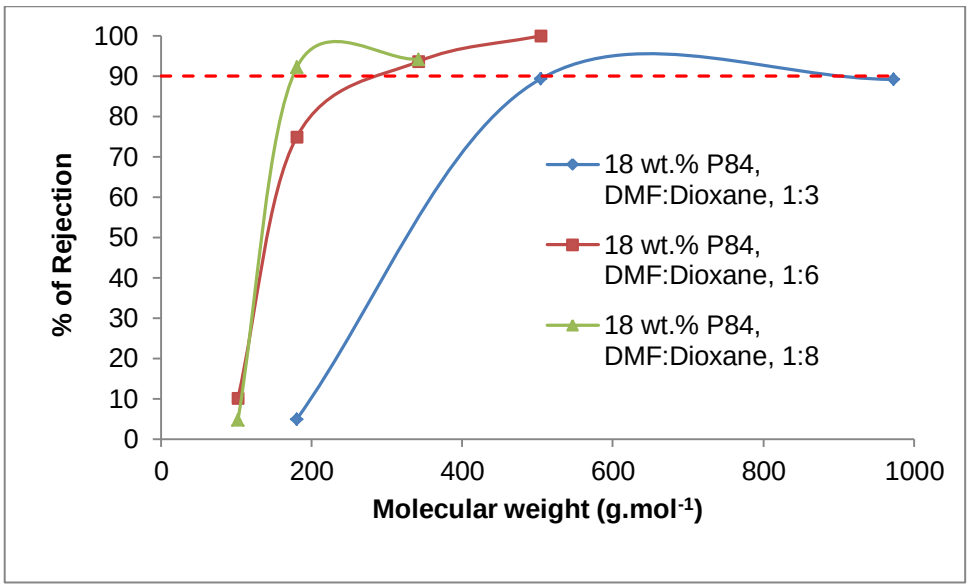

Figure 25-Rejection performance of the membranes 18 wt.% P84 prepared with DMF:Dioxane, 1:3, 1:6 and 1:8.

Table 15 - MWCO 18 wt.%P84 prepared with DMF:Dioxane, 1:3, 1:6 and 1:8.

Membrane composition	MWCO ($g.mol^{-1}$)
18 wt.% P84, DMF:Dioxane - 1:3	≈ 504.2
18 wt.% P84, DMF:Dioxane - 1:6	310.8
18 wt.% P84, DMF:Dioxane - 1:8	178.3

In table 15 we can see that the solvent/co-solvent ratio plays an important role in membrane performance. The results show that the higher the amount of co-solvent in the casting solution, the lower the MWCO of the resulting membranes.

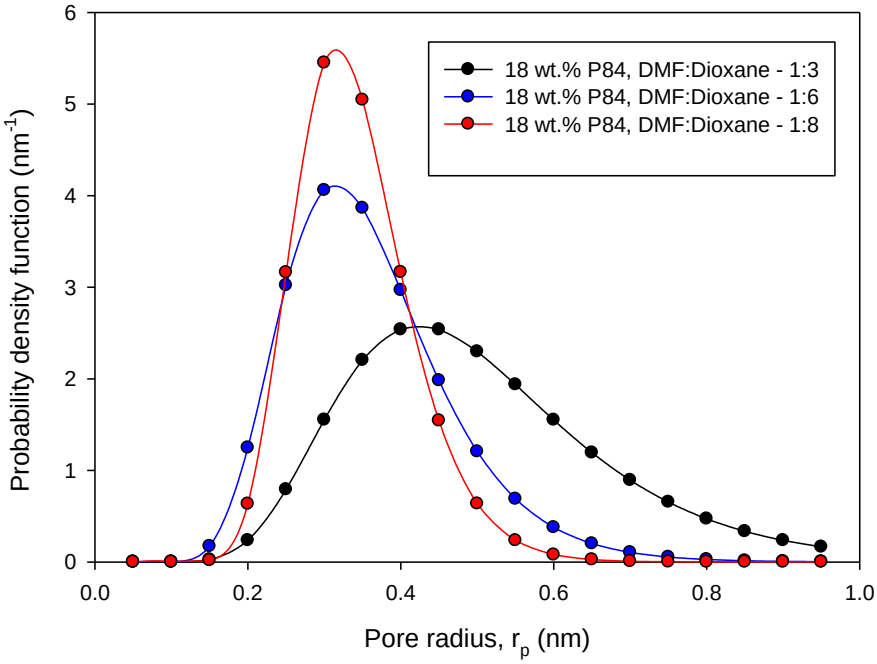

Figure 26- Pore size distribution probability density curves of membranes 18 wt.% P84 prepared with DMF:Dioxane 1:3, 1:6 and 1:8.

Figure 26 shows the pore size distribution of 18 wt.% at DMF:Dioxane ratios of 1:3, 1:6 and 1:8. From Figure 26 we can observe that the increase of co-solvent leads to a lower mean pore size, as well as to a sharper pore size distribution, which is essential for ion rejection.

4.3. ICP effect on membranes performance

To evaluate the severity of ICP effect on the membranes fabricated, the membranes pure water permeability (P) was determined by NF experiments at 10 bar. Assuming that the pure water permeability determined is a membrane constant and σ = 1, and assuming that the full osmotic driving force (bulk osmotic pressure difference) referred as theoretical osmotic driving force, can be realized, a FO theoretical water flux can be calculated based on Eq.10.

$$J_w = P\ \sigma\Delta\pi - \Delta P \quad \textbf{Eq. 10}$$

By dividing this theoretical water flux (the water flux theoretically expected in FO) by the experimental water flux measured, it is obtained the membrane performance ratio. This ratio is equivalent to the bulk osmotic pressure difference that is effectively generating water flux across the FO membrane.

Table 16-The variation of the performance ratio with membrane composition.

Membrane composition	Pure water permeability ($L.m^{-2}.bar^{-1}.h^{-1}$)	Exp. water permeability in FO ($L.m^{-2}.bar^{-1}.h^{-1}$)	Theoretical FO flux ($L.m^{-2}.h^{-1}$)	Exp. FO water flux ($L.m^{-2}.h^{-1}$)	Performance ratio
P84 wt.% 16% DMF:Dioxane 1:3	6,9	0,396	88,3	5,07	0,057
P84 wt.% 18% DMF:Dioxane 1:3	9,2	0,264	117,8	3,37	0,029
P84 wt.% 18% DMF:Dioxane 1:6	6,7	0,465	85,8	5,95	0,069
P84 wt.% 18% DMF:Dioxane 1:8	0,835	0,226	10,7	2,9	0,271
P84 wt.% 20% DMF:Dioxane 1:6	0,734	0,255	9,4	3,26	0,347

Table 16 resumes the pure water permeability determined at 10 bar in a NF cell, the water permeability in FO, the theoretical FO flux determined by Eq.10, the experimental FO water flux measured and the performance ratio for membranes, 16 wt.% P84, DMF:Dioxane, 1:3, 18 wt.% P84, DMF:Dioxane, 1:3, 1:6 and 1:8 an 20 wt.% P84 , DMF:Dioxane, 1:6.

From table 16, we can observe that the tightest membranes, 18 wt.% P84, DMF:Dioxane, 1:8 and 20 wt.% P84 , DMF:Dioxane, 1:6, which MWCO are 178.3 $g.mol^{-1}$ and 178.7 $g.mol^{-1}$ respectively, show the higher performance ratio. Whereas, the membranes with higher MWCO's show performance ratios much lower (≈ 10×lower). This may be explained by the lower water fluxes of the tighter membranes in FO process.

4.4. Ternary phase diagram

The ternary phase diagram (solvent system/ non-solvent/polymer) was plotted in order to study the effect of the solvent system and polymer concentration of a dope solution on phase inversion process.

Dope solutions of 16, 18 and 22 wt.% P84 at different solvent/co-solvent ratios were used to plot the ternary phase diagram.

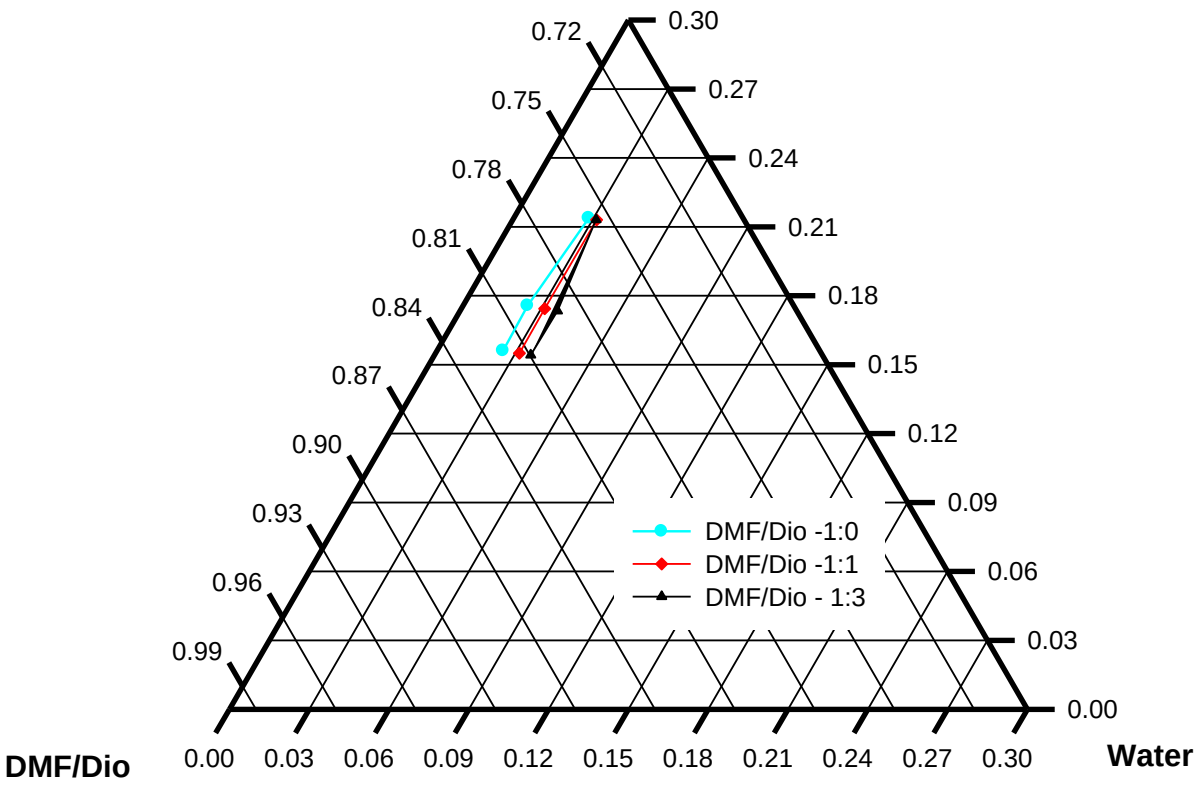

Figure 27- Ternary diagram of P84 at different DMF:Dio ratios.

The amount of non-solvent (water) needed to promote turbidity in a dope solution depends mainly on the solvent system as can be observed in Figure 27. In other words, a particular solvent system requires a similar quantity of water at different polymer concentrations. However, on ternary diagram we can see that the polymer precipitation curve moves towards water/P84 axis at higher dioxane content in the solvent system, which indicates slow demixing during phase inversion.

4.5. Effect of the conditioning agent on membrane performance

To prevent membrane pores from collapsing upon drying, they are usually stored in a conditioning agent after phase inversion. In this work we studied the effect of two conditioning agents on membranes performance in FO process. Therefore, after phase inversion we immersed some of our membranes in aqueous solutions of 40% and 50% polyethylene glycol (400 $g.mol^{-1}$) and glycerol respectively for 12 h. Then, we let the membranes to dry at room temperature and we tested them in FO. The results are shown in tables 18 and 19.

Table 17- Chemical structure, molecular weight and viscosity of glycerol and PEG.

	Glycerol	Polyetilene glycol (PEG 400)
Chemical structure	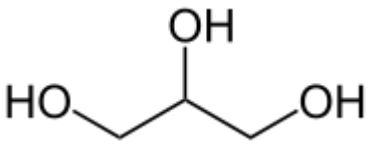	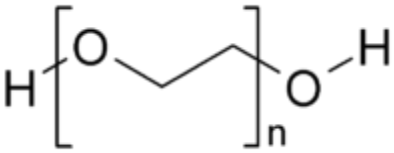
Molecular Weight ($g.mol^{-1}$)	90.1	400
Viscosity (cp) at 25 ºC	1200	90

Table 18- FO performance of membranes stored in PEG compared to those stored in water.

Membrane composition	Storage agent	Flux ($kg.m^{-2}.h^{-1}$)	Permeability ($kg.m^{-2}.bar.h^{-1}$)	% R (Na)
P84 wt.% 18% DMF:Dioxane 1:3	Water	3.37	0.107	89.7%
P84 wt.% 18% DMF:Dioxane 1:3	PEG	4.47	0.142	90.4%
P84 wt.% 18% DMF:Dioxane 1:6	Water	5.95	0.189	87.1%
P84 wt.% 18% DMF:Dioxane 1:6	PEG	5.57	0.177	91.5%
P84 wt.% 18% DMF:Dioxane 1:8	Water	3.40	0.108	92.0%
P84 wt.% 18% DMF:Dioxane 1:8	PEG	1.21	0.038	94.4%

*All experiments were done at least twice and the results shown are an average of the results obtained in each experiment.

Table 19- FO performance of membranes stored in Glycerol compared to those stored in water.

Membrane composition	Storage agent	Flux ($kg.m^{-2}.h^{-1}$)	Permeability ($kg.m^{-2}.bar.h^{-1}$)	% R (Na)
P84 wt.% 18% DMF:Dioxane 1:3	Water	3.37	0.107	89.7%
P84 wt.% 18% DMF:Dioxane 1:3	Glycerol	3.94	0.125	93.4%
P84 wt.% 18% DMF:Dioxane 1:6	Water	5.95	0.189	87.1%
P84 wt.% 18% DMF:Dioxane 1:6	Glycerol	4.76	0.151	92.2%
P84 wt.% 18% DMF:Dioxane 1:8	Water	3.40	0.108	92.0%
P84 wt.% 18% DMF:Dioxane 1:8	Glycerol	1.97	0.062	95.2%

*All experiments were done at least twice and the results shown are an average of the results obtained in each experiment.

Tables 18 and 19 show the performance of membranes 18 wt.% P84, DMF:Dioxane, 1:3, 1:6 and 1:8 in FO, after storage in PEG and Glycerol, respectively.

After immersion of membranes in glycerol or PEG, an increase in salt rejection was observed for all membranes tested, since the emollient may be blocking the pores. This increase in salt rejection promoted a slight water flux decrease for all membranes tested, except 18 wt.%, DMF:Dioxane, 1:3, which may due to the larger pore size of this membrane compared to the pore size of the others tested.

Membrane 18 wt.% P84, DMF:Dioxane, 1:6 immersed in PEG showed a flux reduction of 11% in FO, whereas the same membrane immersed in Glycerol showed a flux reduction of 20%. The increase in rejection was practically the same (5% for immersion in PEG and 6% for immersion in Glycerol). This can be explained by the better hygroscopic properties of PEG compared to Glycerol or by its lower viscosity as well.

For membrane 18 wt.% P84, DMF:Dioxane, 1:8, the flux reduction is equally severe for both conditioning agents. The pores of this membrane are so small that they seem to be completely blocked by the conditioning agents.

4.6. Effect of crosslinking time on membrane performance (FO)

The membrane 18 wt.%, DMF: Dioxane, 1:6 showed the best water flux at a reasonable salt rejection. Therefore, we decided to crosslink this membrane to improve its rejection at expense of its flux (crosslinking mechanism illustrated in Figure 28).

The objective of this section was to study the effect of crosslinking time on membrane performance in FO process (Table 20 and Figure 29).

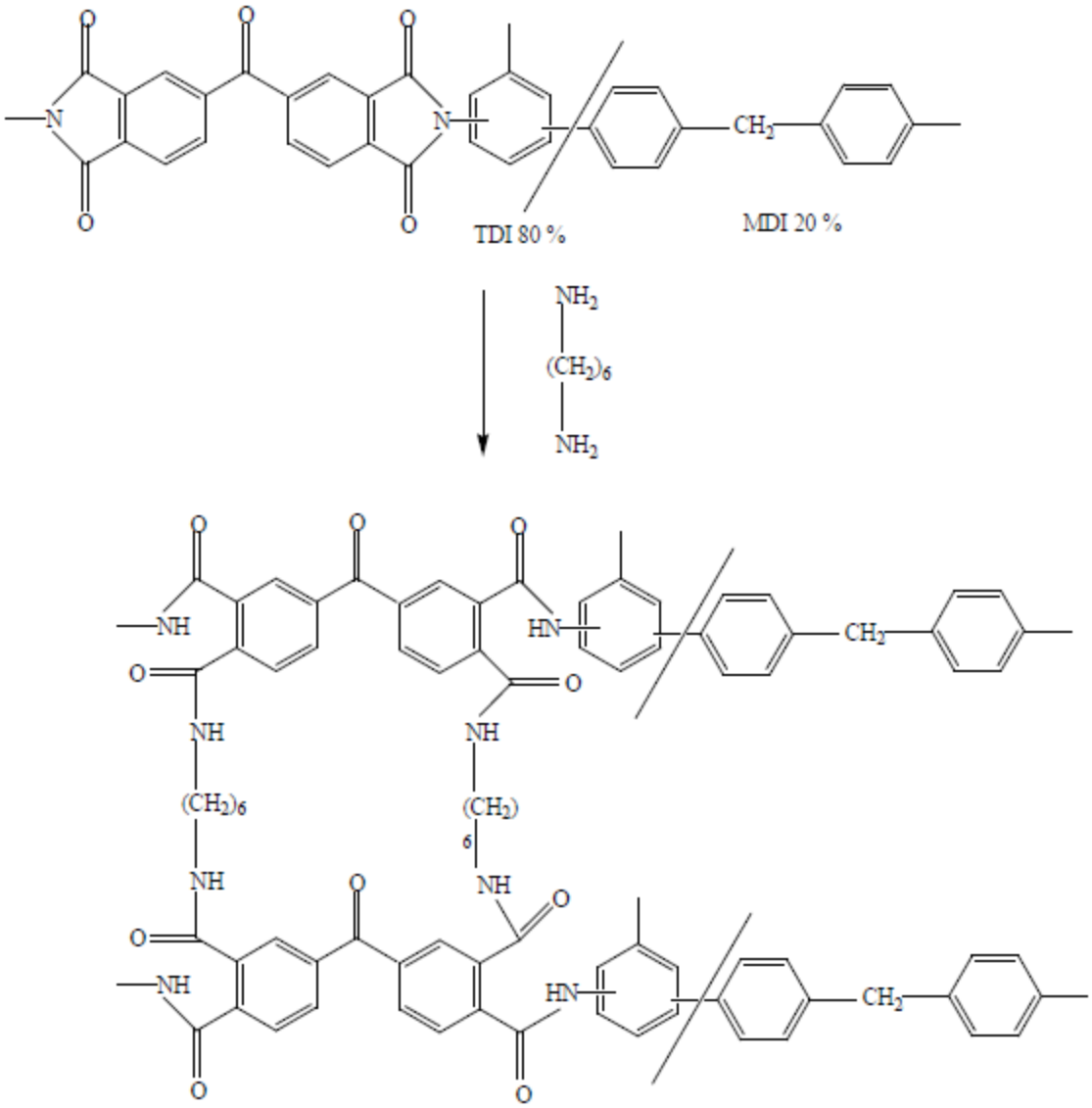

Figure 28- The mechanism of crosslinking of polyimide.

Table 20-Effect of cross linking time on 18 wt.% P84, DMF:Dioxane 1:6 membrane performance in FO.

Entry no	Crosslinking time (h)	Crosslinking agent	Flux ($kg.m^{-2}.h^{-1}$)	Permeability ($kg.m^{-2}.bar.h^{-1}$)	R % (Na)
1*	0	-	5,95	0,465	87,1%
2*	1	HDA	3,57	0,279	91,0%
3	4	HDA	2,18	0,171	95,2%
4	8	HDA	2,03	0,159	94,7%
5*	24	HDA	2,39	0,187	95,4%

*Experiments repeated once. The results shown are an average of the results obtained in each experiment.

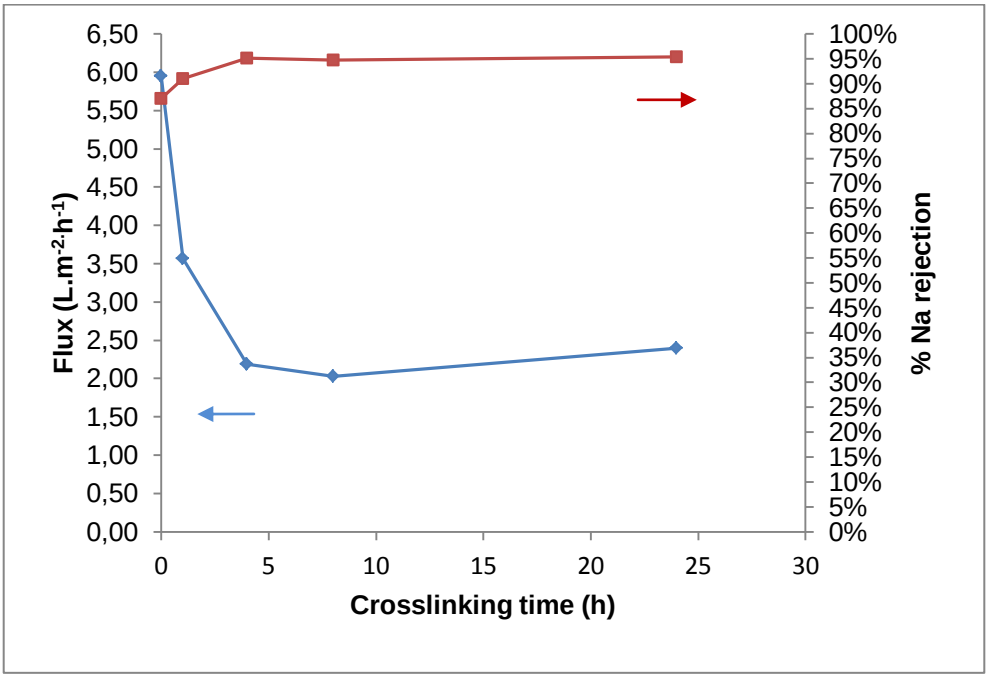

Figure 29-Effect of cross linking time on 18 wt.% P84, DMF:Dioxane 1:6 membrane performance in FO.

The ideal crosslinking time seems to be 4 h, since no big change in flux or rejection is observed for longer crosslinking times. After 4 h of crosslinking, the flux decreased 63.3% and the salt rejection improved 9.3%.

After crosslinking, 18 wt.% P84, DMF:Dioxane, 1:6 shows a flux of 2.18 $L.m^{-2}.h^{-1}$ and a salt rejection of 95%. Comparing this result to Hydration Technology membrane's result, 1.3 $L.h^{-1}.m^{-2}$ with a NaCl rejection of 97 % when tested in the same conditions, it appears that 18 wt.% P84, DMF:Dioxane, 1:6 membrane can be considered a potential membrane for FO. Additionally, improvements on this membrane performance could yet be done by the use of pore forming agents for example.

5. Conclusion remarks and future work

The attention from scientific community has turned toward FO as a new desalination process due to its potential benefits including lower energy consumption, higher feed water recovery and less fouling. However, with the current FO technology these potential benefits were not yet reached. In order to reach these benefits, the development on membrane, draw solute and solute regeneration system must be achieved.

This work explored the potentiality of Polyimide (P84 Lenzing) as a polymer to fabricate a membrane for FO process. Polymer concentrations varying from 14 to 22 wt.% P84 were tried combined with solvent systems varying from pure DMF to DMF:Dioxane, 1:8. The membranes fabricated were tested in FO process and it was observed that membrane polymer concentrations have no big effect on water flux and membrane pore size distribution, but slightly improves membranes salt rejection. On the other hand, the choice of solvent system showed to play the most important role on membrane performance in FO, strongly influencing membranes water flux, salt rejection and pore size distribution. The increase of co-solvent in the casting solution promoted improvement of water flux and salt rejection as well as membranes showing sharper pore size distributions, essential for ion rejection. However, when the amount of co-solvent in the casting solution is too high, membranes become so tight, that its flux drops.

The best performance, in terms of salt rejection and water flux in FO was shown by 18 wt.% P84, DMF:Dioxane, 1:6, which water flux is 5.95 $kg.m^{-2}.h^{-1}$ and salt rejection is 87.1%.

This membrane was later crosslinked by HDA in order to improve its salt rejection at expense of its flux. The best crosslinking time found it was 4h, at which membrane shows a water flux of 2.18 $kg.m^{-2}.h^{-1}$ and a salt rejection of 95.2%. Which means that 18 wt.% P84, DMF:Dioxane, 1:6 membrane can be a potential membrane for FO process, since Hydration Technology membrane, tested in the same conditions showed a water flux of 1.3 $kg.h^{-1}.m^{-2}$ and a salt rejection of 97%.

The performance of the fabricated membranes can yet be improved by the use of pore forming agents and by reducing membranes thickness.

Internal concentration polarisation is thought to be the cause for the lower than expected FO water fluxes obtained. The tighter membranes show performances ratios around 10 times higher than more open membranes. However, at best around 35% of the osmotic pressure driving force is utilized.

In this work, two conditioning agents, Glycerol and PEG were used to store the membranes after phase inversion in order to prevent membrane pores from collapsing upon drying. All membranes stored in aqueous solutions of the conditioning agents showed higher rejection and lower water flux, except 18 wt.%

P84, DMF:Dioxane, 1:3 membrane, which pores are bigger compared to the other membranes subjected to the same conditions. These results may be explained by the pores blockage due to conditioning agent deposition. For 18 wt.% P84, DMF:Dioxane, 1:6 membrane, PEG showed to be the best conditioning agent, promoting lower flux reduction compared to the same membrane stored in glycerol, which could due to PEG lower viscosity.

In future projects, membranes should be casted without the support fabric in order to better understand its influence on membrane performance in terms of water flux, salt rejection and ICP phenomenon. Moreover, other polymers to fabricate membranes should be investigated.

Further investigation in terms of membrane fouling in FO process should also be done, using seawater. FO membranes should also be tested for scale, chlorine, bio and organic fouling.

The development of draw solute with high osmotic efficiency and requiring low energy for regeneration and reconcentration is also as important.

6. References

[1] L.F.Greenlee, D.F. Lawler, Reverse osmosis desalination: Water sources, technology, and today's challenges. Water research 43 (2009) 2317-2348.

[2] S.A. Avlonitis, K. Kouroumbas, N. Vlachakis, Energy consumption and membrane replacement cost for seawater RO desalination plants, Desalination 157 (2003) 151-158.

[3] H. Strathmann, Asymetric polyimide membrane for filtration of non-aqueous solutions,Desalination 26 (1978) 85-91.

[4] I.W. Olney, B.S. Minhas, Asymetric polyimide membranes, US patent 5,067,970 (1991).

[5] M.T. Ravanchi, T.Kaghazchi, Application of membrane separation processes in petrochemical industry: a review, Desalination 235 (2009) 199-244.

[6] T.V. Naylor, Polymer Membranes – Materials, Structures and Separation Performance, Vol. 8, Numb. 5, RAPRA technology ltd ed., 1996.

[7] M. Mulder, Basic Principles of Membrane Technology, 2nd ed. Netherlands, Kluwer Academic Publishers, 1996.

[8] P. Vandezande, L.E.M. Gevers, Solvent resistant nanofiltration: separating on a molecular level, Chemical Society Reviews, 2007.

[9] M. Ishiguro, T.Matsuura, A Study on the Solute Separation and the Pore Size Distribution of a Montmorillonite Membrane, Separation Science and Technology, 31:4 (1996) 545-556.

[10] S.Singh, K.C. Khulbe, Membrane characterization by solute transport and atomic force microscopy, Journal of Membrane Science 142 (1998) 111-127.

[11] S. Nakao, Determination of pore size distribution 3. Filtration membranes, Journal of Membrane Science, 96 (1994) 131-165.

[12] A.S. Michaels, Analysis and prediction of sieving curves for ultrafiltration membranes: A universal correlation?. Sep. Sci. Technol. 15 (1985) 61-76.

[13] A.R. Cooper, D.S. Van Derveer, Characterization of ultrafiltration membranes by polymer transport measurement, Sep. Sci. Technol. 14 (1979) 551-556.

[14] M. Ishiguro, T. Matsuura, A study on the solute separation and the pore size distribution of a montmorillointe membrane, Sep. Sci. Tecchnol. 31 (1996) 545-556.

[15] W.R. Bowen, A.W. Mohammad, Characterization and prediction of Nanofiltration membrane performance – a general assessment, Trans. IChemE. Part A 76 (1998) 885.

[16] K.Y. Wang, T. Chung, Polybenzimidazole (PBI) nanofiltration hollow fiber membranes process, Journal of Membrane Science 300 (2007) 6-12.

[17] S. Loeb and S. Sourirajan, Adv. Chem. Ser.,38 (1963) 117.

[18] H.J. Lee, B. Jung, Phase separation of polymer casting solution by non-solvent vapour, Journal of Membrane Science 245 (2004) 103-112.

[19] H. Strathamann, K. Kock, The formation Mechanism of phase inversion membranes, Desalination, 21 (1977) 241-255.

[20] F.G. Paulsen, S.S. Shojaie, Effect of evaporation step on macrovoid formation in wet-cast polymeric membranes, Journal of Membrane Science 91 (1994) 265-282.

[21] Y.H. See-Tho, M.Silva, Controlling molecular weight cut-off curves for high solvent stable organic solvent nanofiltration (OSN) membranes, Journal of Membrane Science, 324 (2008) 220-232.

[22] F.W. Altena, C.A. Smolders,Macromolecules, 15 (1982) 1491.

[23] A.J. Reuvers, Ph.D. Thesis, University of Twente, 1987.

[24] N.A. Mohamad, Polymer, 38 (1997) 4705.

[25] M. Han, D. Bhattacharyya, Thermal annealing effect on cellulose acetate reverse osmosis membrane structure, Desalination 101 (1905) 195.200.

[26] Y.H. See-Toh, F.C. Ferreira, The influence of membrane formation parameters on the functional performance of organic solvent nanofiltration membranes, Journal of Membrane Science 299 (2007) 236-250.

[27] I.C. Karagiannis, P.G. Soldatos, Water desalination cost literature: review and assessment, Desalination, 223 (2008) 448-456.

[28] HYDRANAUTICS, High Performance Membrane Products, A Nitto Denko Corporation.

[29] K.D. Vos, A.P. Hatcher, U. Merten, Lifetime of cellulose acetate reverse osmosis membranes, Ind. Eng. Chem. Prod. Res. Devel., 5 (1966) 211-218.

[30] G. Kang, C.Gao, Study on hypochlorite degradation of aromatic polyamide reverse osmosis membrane, Desalination, 32 (1980) 25-31.

[31] R.Elinav, K. Harussi, The footprint of the desalination processes on the environment, Desalination, 152 (2003) 141-154.

[32] A.M. Alklaibi, N.Lior, Membrane-distillation desalination: status and potential, Desalination 171 (2004) 111-131.

[33] J.L.M.C.Martins, master thesis, University Nova de Lisboa, 2010.

[34] S. Al-Obaidani, E. Curcio, Potential of membrane distillation in seawater desalination: Thermal efficiency sensitivity study and cost estimation, Journal of Membrane Science, 323 (2008) 85-98.

[35] T.Y. Cath, A. E. Childress, Forward Osmosis: Principles, applications, and recent developments, Journal of Membrane Science 281 (2008) 70-87.

[36] A. Achilli, T.Y. Cath, The forward osmosis membrane bioreactor: A low fouling alternative to MBR processes, Desalination 239 (2009) 10-21.

[37] H.F. Ridgway, Biological Fouling of Separation Membranes used in Water Treatment Applications, AWWA Research Foundation (2003).

[38] K. Anthony, Osmotic Power ahead?, Chemestry and Industry, (21 June 2010) 24-27.

[39] J.R. McCutcheon, R.L.McGinnins, A novel ammonia-carbon dioxid forward (direct) desalination process,Desalination 174 (2005) 1-11.

[40] G.W. Batchelder, Process for the Demineralizaion of water, US patent 3,171,799 , 1965.

[41] D.N. Glew, Process for liquid recovery and solution concentration, US Patent 3,216,930, 1965.

[42] B.S. Frank, Desalination of sea water, US Patent 3,670,897, 1972.

[43] J.O. Kessler, C.D. Moody, Drinking water from sea water by forward osmosis, Desalination 18 (1976) 297–306.

[44] R.E. Kravath, J.A. Davis, Desalination of seawater by direct osmosis, Desalination 16 (1975) 151–155.

[45] R.L. McGinnis, Osmotic desalination process (1), US patent 6,391,205 B1, 2002.

[46] J.R. McCutcheon, R.L. McGinnis, Desalination by ammonia-carbon dioxide forward osmosis: Influence of draw and feed solution concentrations on process performance, Journal of Membrane Science, 278 (2006) 114-123.

[47] R.L. McGinnis, M. Elimelech, Energy Requirements of ammonia-carbon dioxide forward osmosis desalination, Desalination 207 (2007) 370-382.

[48] NanoMagnetics, Water purification, 2005. Electronic Source: http://www.nanomagnetics.com/water purification.asp.

[49] S. Loeb, L. Titelman, E. Korngold, J. Freiman, Effect of porous support fabric on osmosis through a Loeb–Sourirajan type asymmetric membrane, J. Membr. Sci. 129 (1997) 243–249.

[50] G.T. Gray, J.R.McCutcheon, Internal concentration polarization in forward osmosis: role of membrane orientation, Desalination 197 (2006) 1-8.

[51] G.D. Mehta, S.Loeb. Performance of Permasep B-9 and B-10 membranes in various regions and at high osmotic pressure, Hournal of Membrane Science, 4 (1979) 335-349.

[52] J.R. McCutcheon, M. Elimelech, Influence of concentrative and dilutive internal concentration polarization on flux behavior in forward osmosis, Journal of Membrane Science 284 (2006) 237-247.

[53] E.M.Garcia-Castello, J.R.McCutcheon, Performance evaluation of sucrose concentration using forward osmosis, Journal of Membrane Science 338 (2009) 61-66.

[54] R. Wang, L.Shi, Characterization of novel forward osmosis hollow fiber membranes, Journal of Membrane Science, 355 (2010) 158-167.

[55] K.Y.Wang, Q.Yang, Enhanced forward osmosis from chemically modified polybenzimidazole (PBI) nanofiltration hollow fiber membranes with a thin wall, Chemical Engineering Science 64 (2009) 1577.1584.

[56] K.Vanherck, A.Cano-Odena, A simplified diamine crosslinking method for PI nanofiltration membranes, Journal of Membrane Science, 353 (2010) 135-143.

[57] I.Soroko, A. Livingston, Impact of TIO_2 nanoparticles on morphology and performance of crosslinked polyimide organic solvent nanofiltration (OSN) membranes, Journal of Membrane Science, 343 (2009) 189.198.

[58] Y.C. Wang, *Sorption and transport properties of gases in aromatic polyimide membrane,* Journal of Membrane Science, 248(2005)15-25.

[59] M.P. Lopes, master thesis, University Nova de Lisboa, 2009.

7. Attachment

7.1. SEM pictures of the membranes fabricated

- P84 18 wt.%**, 82 wt.% DMF**

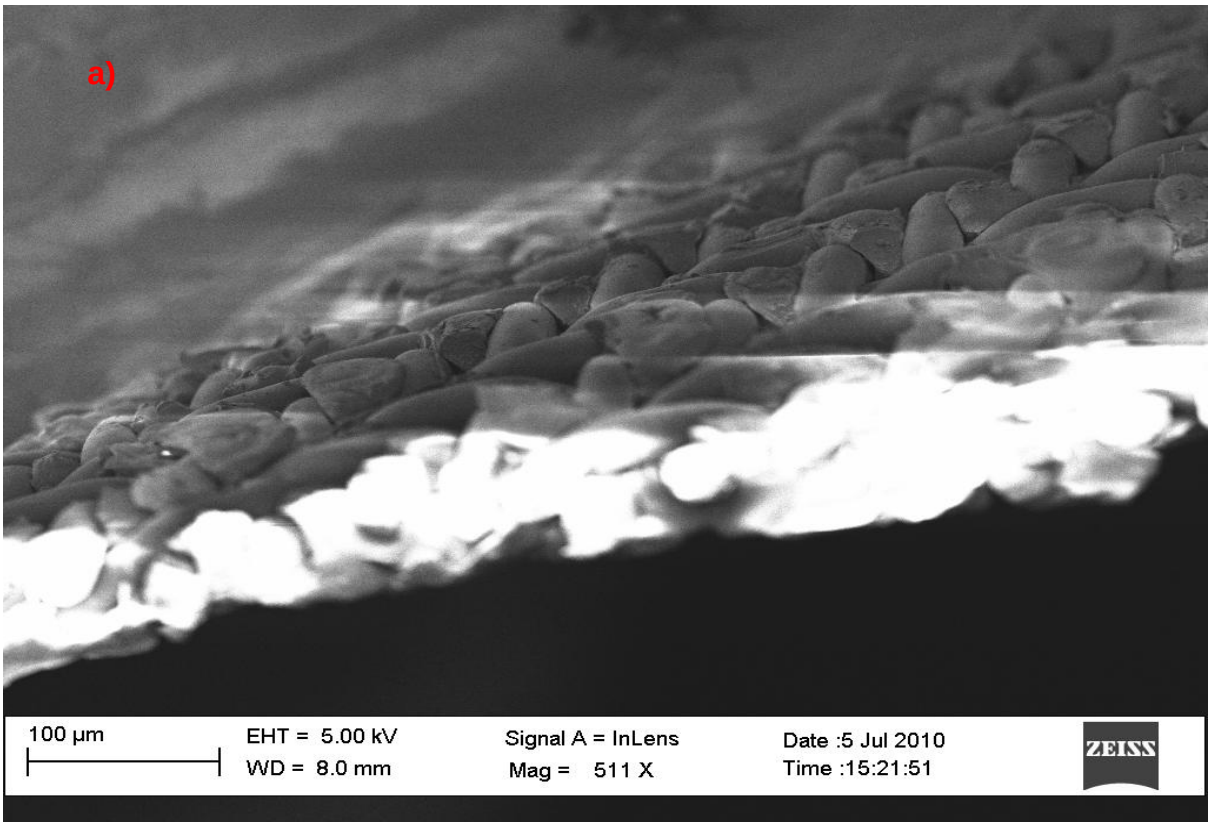

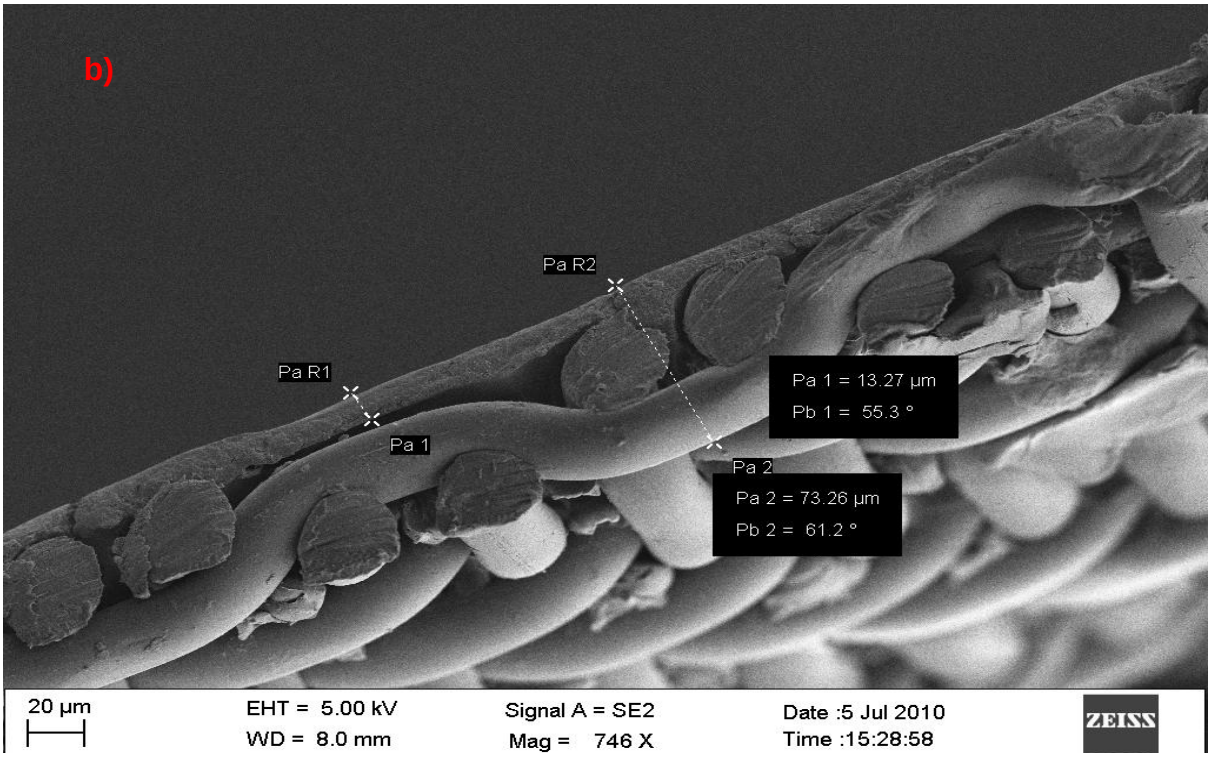

Figure 30-SEM pictures of membrane 18 wt.%, 82% DMD. a) backside of the membrane; b) Cross-section of the membrane.

- P84 18 wt.%**, 1:3 DMF:Dio**

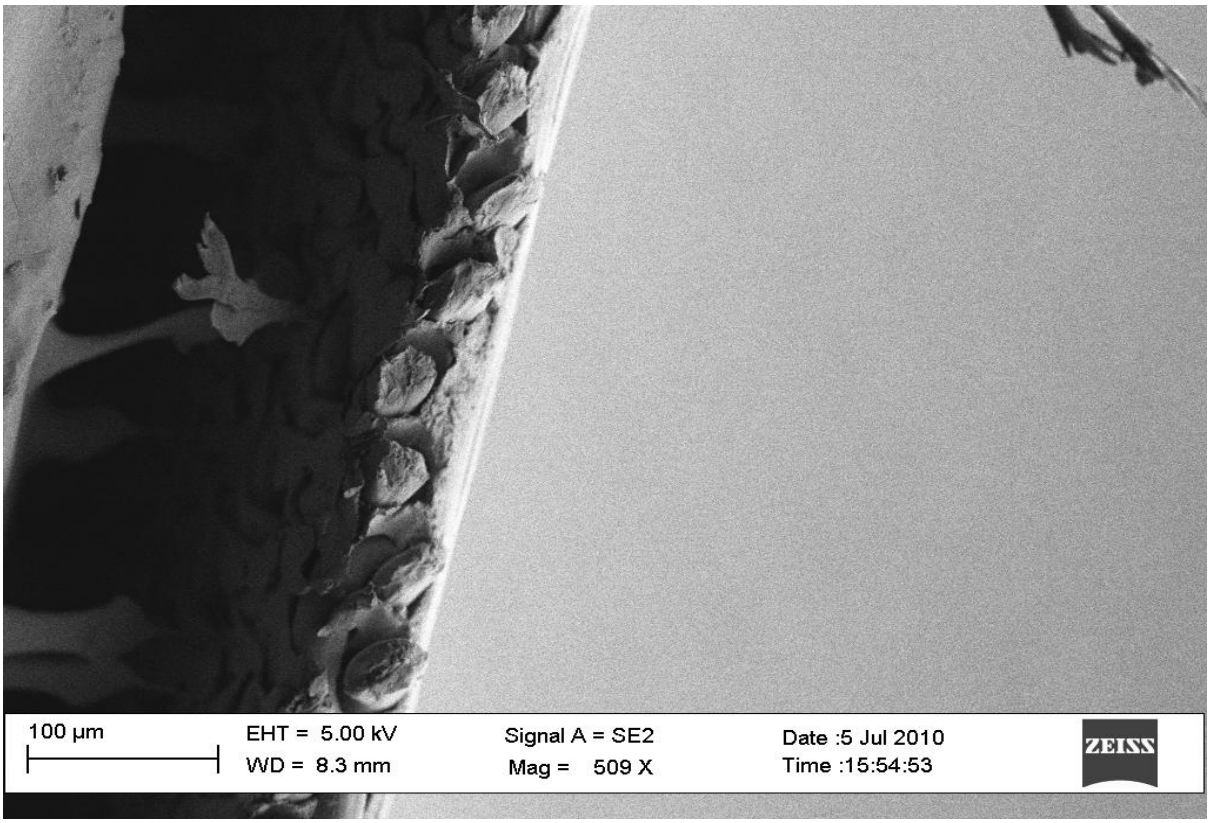

Figure 31 - Cross-section of membrane 18 wt.%, 1:3 DMF:Dio.

- P84 18 wt.%**, 1:6 DMF:Dio**

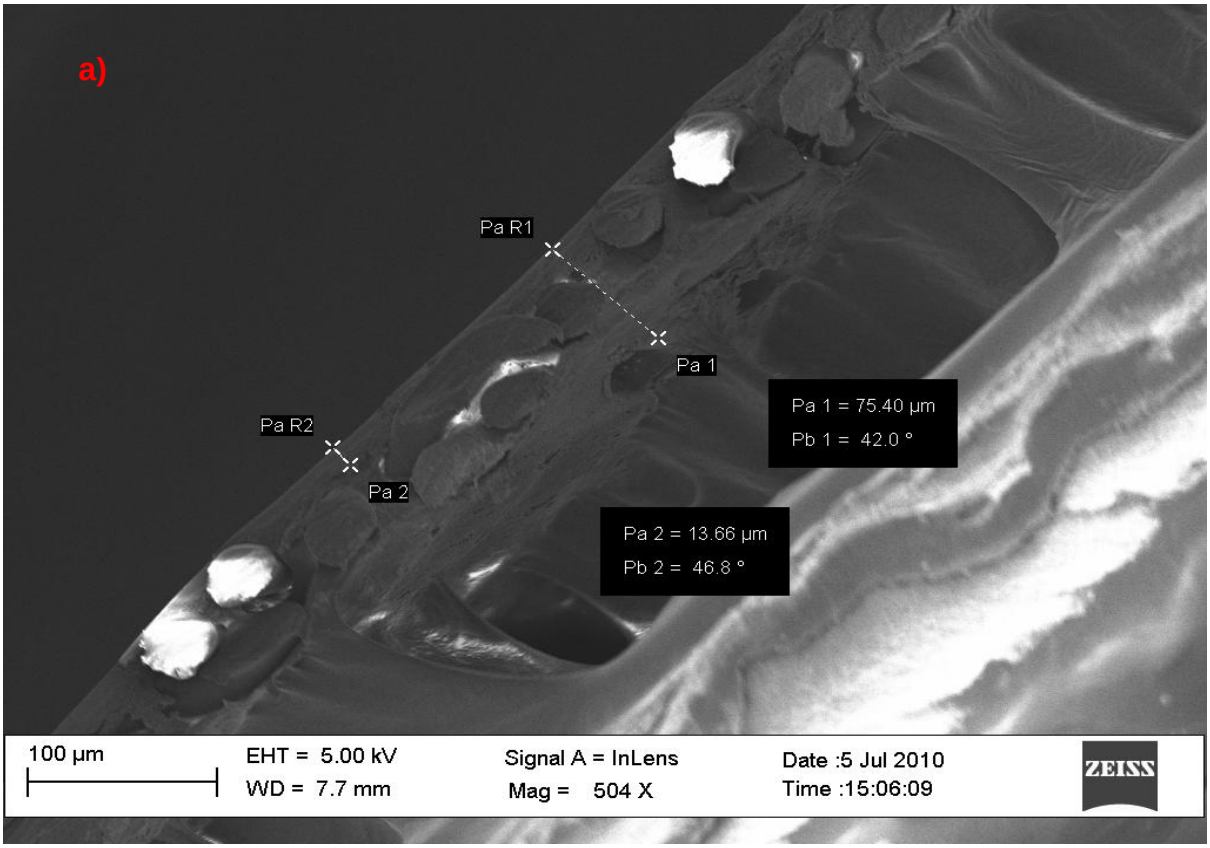

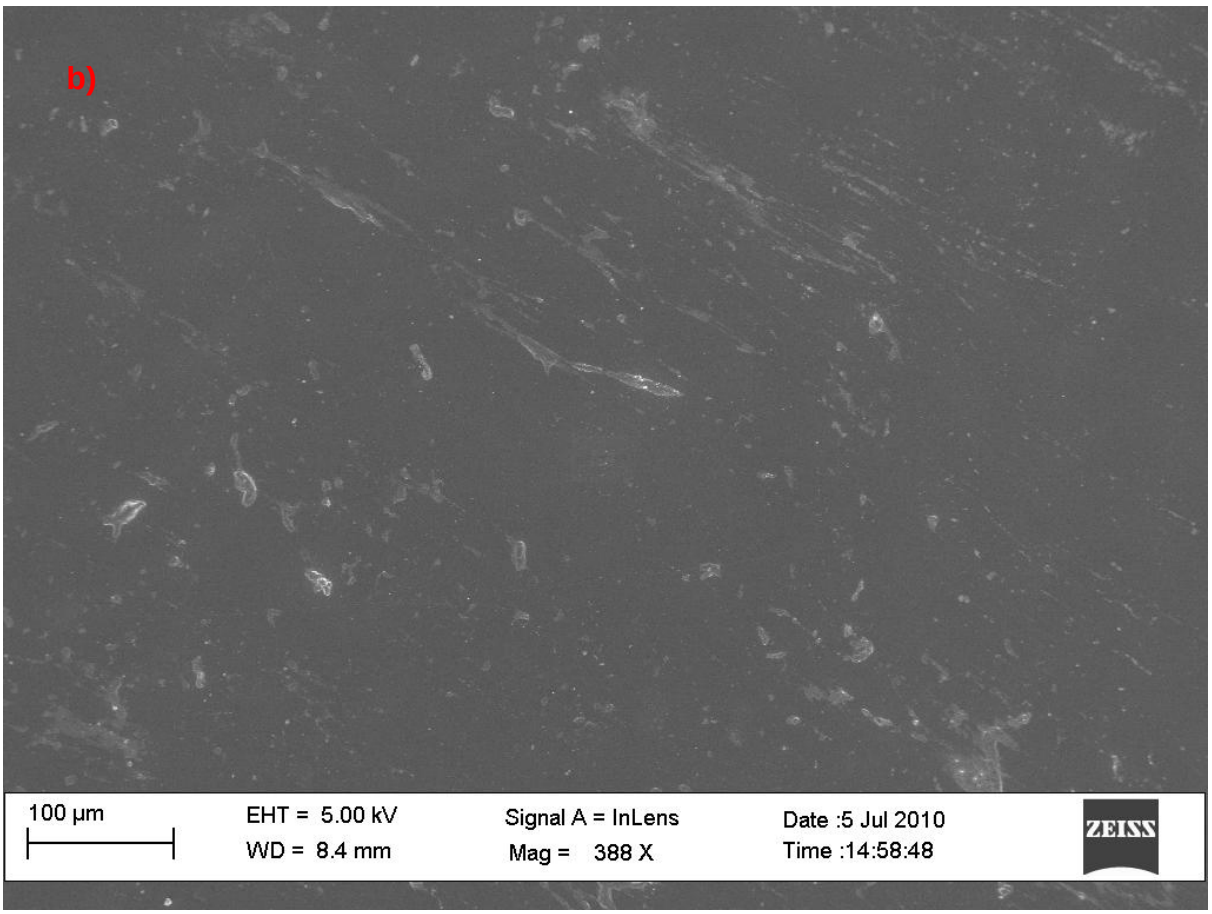

Figure 32 - SEM pictures of membrane 18 wt.%, 1:6 DMF:Dio. a) Cross-section of the membrane; b) Surface of the membrane.

- P84 18 wt.%**, 1:8 DMF:Dio**

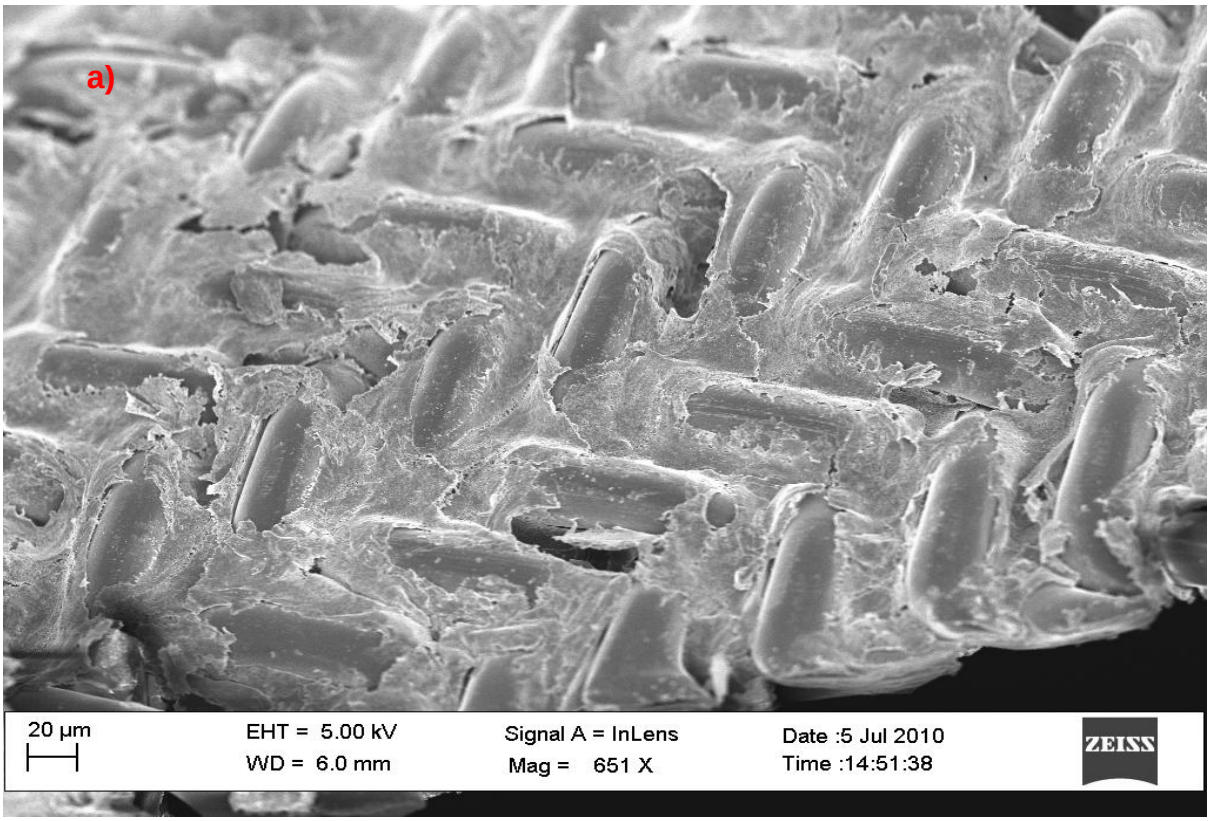

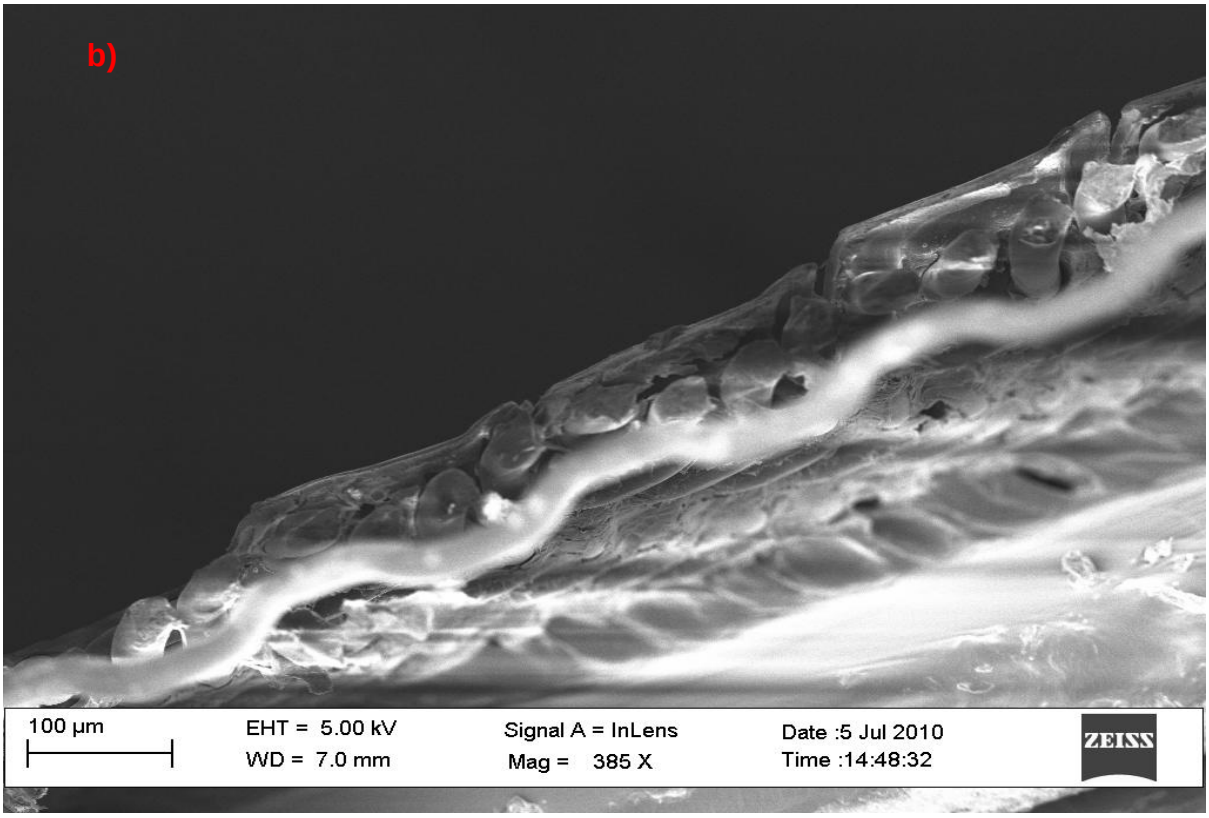

Figure 33-SEM pictures of membrane 18 wt.%, 1:8 DMF:Dio. a) Backside of the membrane; b) Cross-section of the membrane

- **P84 16 wt.%,** 1:6 DMF:Dio

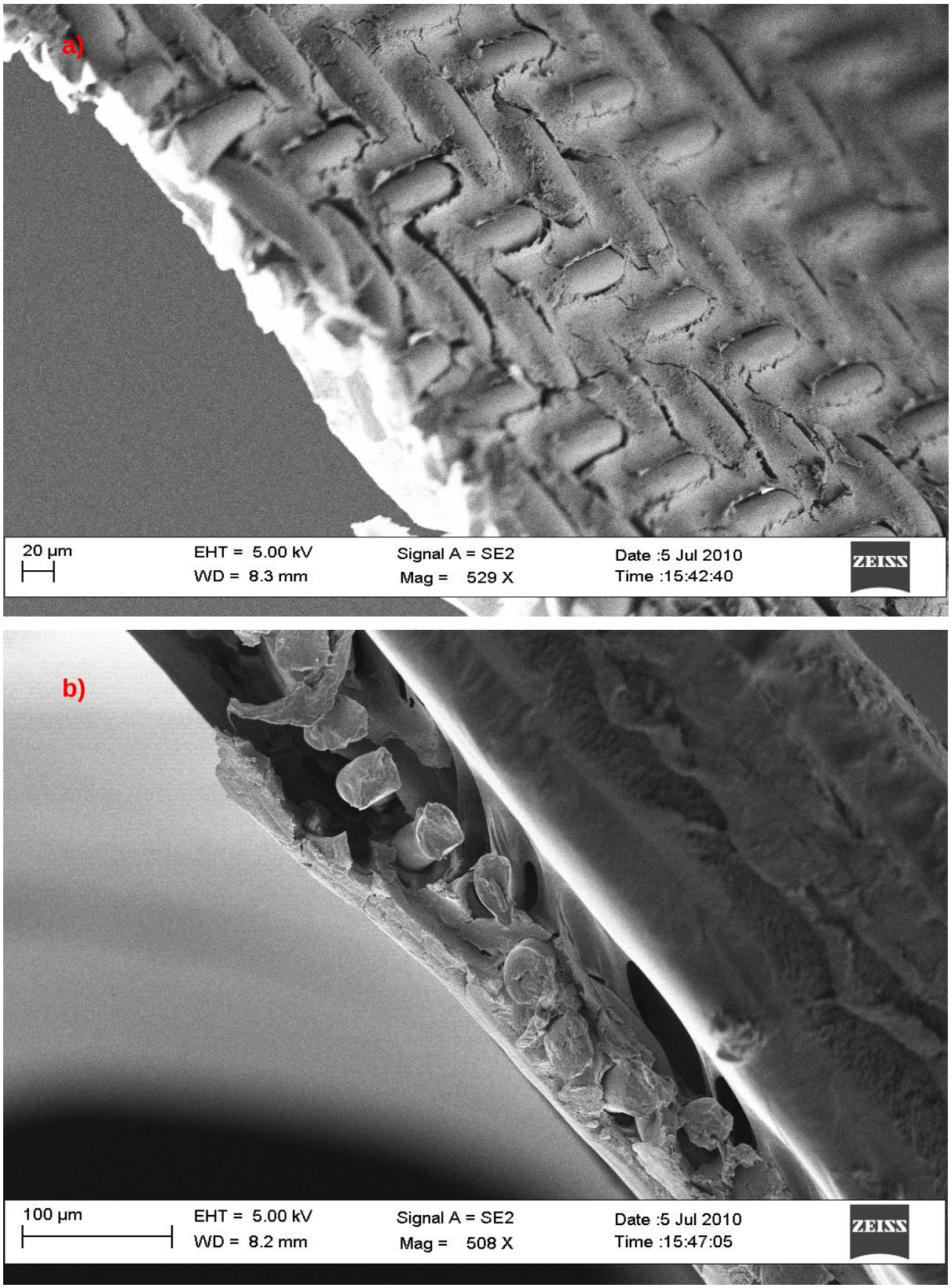

Figure 34 - SEM pictures of membrane 16 wt.%, 1:6 DMF:Dio. a) Backside of the membrane; b) Cross-section of the membrane

- **P84 20 wt.%,** 1:6 DMF:Dio

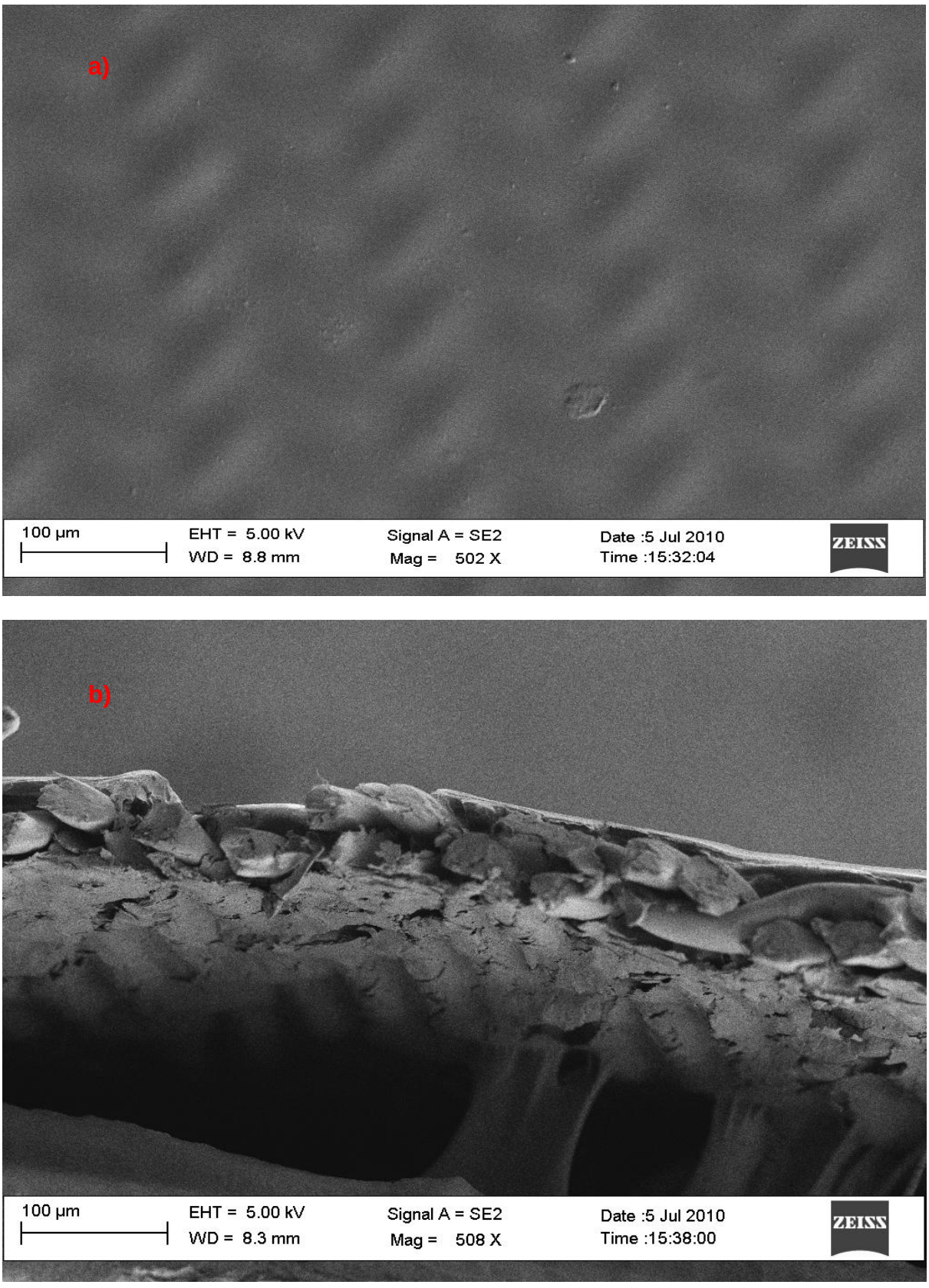

Figure 35 - SEM pictures of membrane 16 wt.%, 1:6 DMF:Dio. a) Surface of the membrane; b) Cross-section of the membrane.